

Supporting Information

Simple pyridyl-salicylimine-based fluorescence “turn-on” sensors for distinct detections of Zn^{2+} , Al^{3+} and OH^- ions in mixed-aqueous media

Muthaiah Shellaiah, Yen-Hsing Wu and Hong-Cheu Lin*

Department of Materials Science and Engineering, National Chiao Tung University,
Hsinchu 30049, Taiwan (ROC)

*Correspondence should be addressed to

E-mail: linhc@mail.nctu.edu.tw

Fax: +8863-5724727; Tel: +8863-5712121 ext.55305

Table contents:

Experimental section (S2-S3)

^1H NMR, ^{13}C NMR and mass (FAB) scanned spectra of F1, F2 and F3 (S3-S8)

PL spectral responses of F1, F2 and F3 as a function of pH (S8)

Fluorescence and time resolved photoluminescence spectra (TRPL) of F1, F2 and F3 at acidic, neutral and basic pHs (2, 7 and 12) (S9-S10)

Computation analysis of HOMO-LUMO of F1, F2 and F3 (Semi empirical method) (S11)

Sensor responses, of F1, F2 and F3 in $\text{CH}_3\text{CN}/\text{H}_2\text{O}$ (3/7) towards Al^{3+} ions in H_2O (S12)

UV-Vis titrations of F1 and F2 towards Zn^{2+} ions (S13)

UV-Vis titrations of F1, F2 and F3 in $\text{CH}_3\text{CN}/\text{H}_2\text{O}$ (6/4 and 3/7) towards Al^{3+} ions (S14)

Fluorescence spectra and histograms of sensor responses of F1, F2 and F3 $\text{CH}_3\text{CN}/\text{H}_2\text{O}$ (3/7) towards Al^{3+} ions in H_2O (S15-S16)

Comparison of relative fluorescence intensity changes of F1, F2, and F3 in $\text{CH}_3\text{CN}/\text{H}_2\text{O}$ (6/4 and 3/7) towards Zn^{2+} , Al^{3+} and OH^- ions in H_2O (S17)

Fluorescence and UV-Vis titrations and histograms of F1, F2 and F3 towards OH^- ions (S18-S20)

Stoichiometry calculation of F1, F2 and F3 to Zn^{2+} and Al^{3+} ions (S21)

^{13}C NMR spectral changes towards sensor responses of F1, F2 and F3 (S22-S29)

Mass (FAB) spectral changes towards sensor responses of F1, F2 and F3 (S30-S33)

Sensor reversibilities of $\text{F1}+\text{Zn}^{2+}$ and $\text{F2}+\text{Zn}^{2+}$ (S34)

Detection limits (LODs) calculations of F1, F2 and F3 towards Zn^{2+} , Al^{3+} and OH^- ions (S35-S36)

^{13}C NMR and mass (FAB) spectral changes of ratiometric displacements of $\text{F1}+\text{Zn}^{2+}$ and $\text{F2}+\text{Zn}^{2+}$ by Al^{3+} ions (S37-S39)

Response parameter values (α) of metal sensor complexes of F1, F2 and F3 (S40-S41)

TRPL spectra of sensor complexes of F1, F2 and F3 (S42)

Fluorescence spectral responses of F1, F2, F3 and their sensor complexes with respect to water concentration, pH and time/minutes (S43-S45)

^1H NMR, PL titrations LOD calculations and TRPL spectra of F1, F2 and F3 towards Ga^{3+} ions (S46-S49)

TRPL and photophysical properties (Table S1 and S2) of F1, F2, F3 and their sensor responses (S50-S51)

Experimental section

General information

All anhydrous reactions were carried out by standard procedures under nitrogen atmosphere to avoid moisture. The solvents were dried by distillation over appropriate drying agents. Reactions were monitored by TLC plates and column chromatography was generally performed on silica gel. ^1H and ^{13}C -NMR were recorded on a 300 MHz spectrometer. The chemical shifts (δ) are reported in ppm and coupling constants (J) in Hz and relative to TMS (0.00) for ^1H and ^{13}C . R, (s, d, t, q, m, and br mean single, double, ternary, quadruple, multiple, and broad single, respectively), and d-chloroforms (7.26) & (77.0) were used as references for ^1H and ^{13}C NMR, respectively. Mass spectra (FAB) were obtained on the respective mass spectrometer. Elemental analysis was carried out by Elemental Vario EL. Absorption and fluorescence spectra were measured on V-670 spectrophotometer and F-4500 fluorescence spectrophotometer, respectively. Fargo Mp-2D melting point apparatus was used to measure the melting ranges of all solid compounds. Identification and purity of the compounds **F1**, **F2** and **F3** were characterized by NMR (^1H & ^{13}C), Mass (FAB), and melting point measurements. Time-resolved photoluminescence (TRPL) spectra were measured using a home-built single photon counting system. Excitation was performed using a 350 nm diode laser (Picoquant PDL-200, 50 ps fwhm, 2 MHz). The signals collected at the excitonic emissions of solutions were connected to a time-correlated single photon counting card (TCSPC, Picoquant Timeharp 200). The emission decay data were analyzed with the biexponential kinetics in which two decay components were derived. The lifetime values (τ_1 and τ_2) and pre-exponential factors (A_1 and A_2) were determined and summarized. 1-14 pH buffers were freshly prepared as per the literature.¹

Sensor titrations

Compounds **F1**, **F2**, and **F3** were dissolved in $\text{CH}_3\text{CN}/\text{H}_2\text{O}$ (6/4 and 3/7) at 1×10^{-5} M concentration. Li^+ , Ag^+ , K^+ , Na^+ , Cs^+ , Ni^{2+} , Fe^{2+} , Co^{2+} , Zn^{2+} , Cd^{2+} , Pb^{2+} , In^{3+} , Ga^{3+} , Mg^{2+} , Cu^{2+} , Cr^{3+} , Fe^{3+} and Al^{3+} metal cations were dissolved in water medium at 1×10^{-4} M concentration from their respective chloro compounds, and Ag^{2+} , Mn^{2+} , Eu^{3+} , Hg^{2+} and Mg^{2+} were made from AgNO_3 , Mn(OAc)_2 , Eu(OAc)_3 , Hg(OAc)_2 and MgSO_4 , respectively, in water medium at 1×10^{-4} M concentration. (Metal ion mixtures contained all above ions, except Zn^{2+} and Al^{3+} ions). Ethylene diamine tetra acetic acid (EDTA) was dissolved in H_2O at 1×10^{-5} M. All OH^- , BH_4^- , NO_3^- , PO_4^{3-} , ClO_4^- , F^- , Cl^- , Br^- and I^- anions were dissolved in water medium at 1×10^{-3} M from their respective tetra butyl ammonium salts. (Anion mixtures contained all above ions, except OH^- ion).

NMR titrations and mass spectra

1 equiv. of **F1**, **F2** and **F3** in CD_3CN were titrated with 1 equiv. of Zn^{2+} or Al^{3+} in D_2O and also titrated with 1:1 ratiometrically (each 3 equiv.) mixed with Zn^{2+} and Al^{3+} ions in D_2O and those NMR samples were stirred at 70°C for 2 days, after complete evaporation of the solvent it was dried in vacuum at 50°C for 3 hrs. The fine powders obtained were further investigated via Mass (FAB) spectra to confirm the complex formation. Similarly, OH^- anion was investigated by titrating 5 equiv. of tetra butyl ammonium hydroxide (TBAOH) in D_2O with 1 equiv. of **F1** or **F2** or **F3** in CD_3CN , and because of the hygroscopic nature of TBAOH, the NMR samples were immediately analyzed by mass (FAB) spectra without further drying.

General procedure for the synthesis of **F1**, **F2** and **F3**

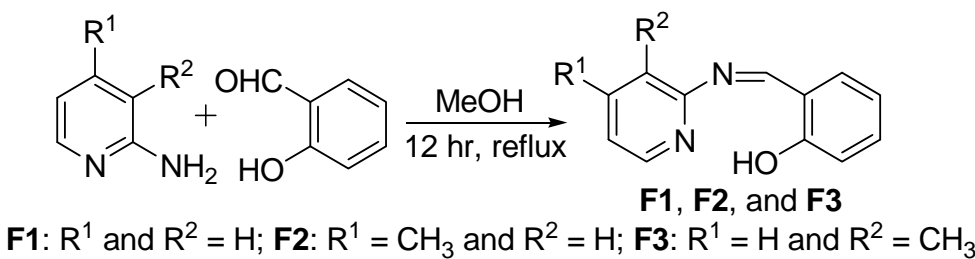
To 1 equiv. of 2-amino pyridyl derivatives [5 g; 53.13 mmol (**F1**) and 46.24 mmol (**F2** and **F3**)] in 50 ml of methanol, 1 equiv. of salicylaldehyde [6.5 g, 53.22 mmol (**F1**) and 5.65 g, 46.26 mmol (**F2** and **F3**)] was added with constant stirring under nitrogen and then refluxed for 12 hrs. The reaction was monitored by TLC. After completion, the reaction mixtures were cooled and the

solvent was evaporated to give the crude products, which were recrystallized from ethanol to afford pure compounds (**F1**, **F2** and **F3**).

2-((pyridin-2-ylimino)methyl)phenol (F1**)**: Dark yellow solid; 10.11 g; 96% yield; M.P = 65-67°C; ¹H NMR (300 MHz, CDCl₃) δ: 6.90 – 7.18 (m, 2H), 7.20 – 7.48 (m, 4H), 7.71 (t, *J* = 9.0 Hz, 1H), 8.47 (d, *J* = 6.0 Hz, 1H), 9.40 (s, 1H), 13.44 (s, 1H (-OH)); ¹³C NMR (300 MHz, CDCl₃) δ: 117.16, 118.89, 119.15, 120.50, 133.41, 133.77, 138.40, 148.86, 157.46, 161.77, 164.66; FAB: m/z = 198 (M⁺, 100%). Anal. Calcd for C₁₂H₁₀N₂O: C, 72.71; H, 5.08; N, 14.13. Found: C, 72.54; H, 5.06; N, 14.12.

2-((4-methylpyridin-2-ylimino)methyl)phenol (F2**)**: Bright yellow crystals; 9.62 g; 98% yield; M.P = 102-104°C; ¹H NMR (300 MHz, CDCl₃) δ: 2.37 (s, 3H), 6.90 – 7.12 (m, 4H), 7.35 – 7.46 (m, 2H), 8.33 (d, *J* = 6.0 Hz, 1H), 9.40 (s, 1H), 13.49 (s, 1H (-OH)); ¹³C NMR (300 MHz, CDCl₃) δ: 20.86, 117.13, 118.91, 119.07, 121.08, 123.55, 133.31, 133.63, 148.47, 149.80, 157.47, 161.77, 164.47; FAB: m/z = 212 (M⁺, 100%). Anal. Calcd for C₁₃H₁₂N₂O: C, 73.56; H, 5.70; N, 13.20. Found: C, 73.50; H, 5.67; N, 13.18.

2-((3-methylpyridin-2-ylimino)methyl)phenol (F3**)**: Bright yellow powder; 9.52 g; 97% yield; M.P = 81-83°C; ¹H NMR (300 MHz, CDCl₃) δ: 2.49 (s, 3H), 6.96 – 7.19 (m, 3H), 7.53 – 7.61 (m, 3H), 8.36 (d, *J* = 6.0 Hz, 1H), 9.43 (s, 1H), 13.79 (s, 1H (-OH)); ¹³C NMR (300 MHz, CDCl₃) δ: 17.65, 117.17, 119.14, 122.61, 124.71, 128.50, 133.38, 133.76, 139.48, 146.31, 155.79, 162.01, 163.87; FAB: m/z = 212 (M⁺, 100%). Anal. Calcd for C₁₃H₁₂N₂O: C, 73.56; H, 5.70; N, 13.20. Found: C, 73.52; H, 5.68; N, 13.19.



Scheme S1 Synthesis of **F1**, **F2** and **F3**.

References

- (1) R. A. Robinson, R. H. Stokes, "Electrolyte solutions" 2nd ed., rev. 1968, London, Butterworth.
- (2) G. Gryniewicz, M. Poenie and R. Y. Tsein, *J. Biol. Chem.*, 1985, **260**, 3440.
- (3) D. Maity and T. Govindaraju, *Chem. Commun.*, 2012, **48**, 1039.

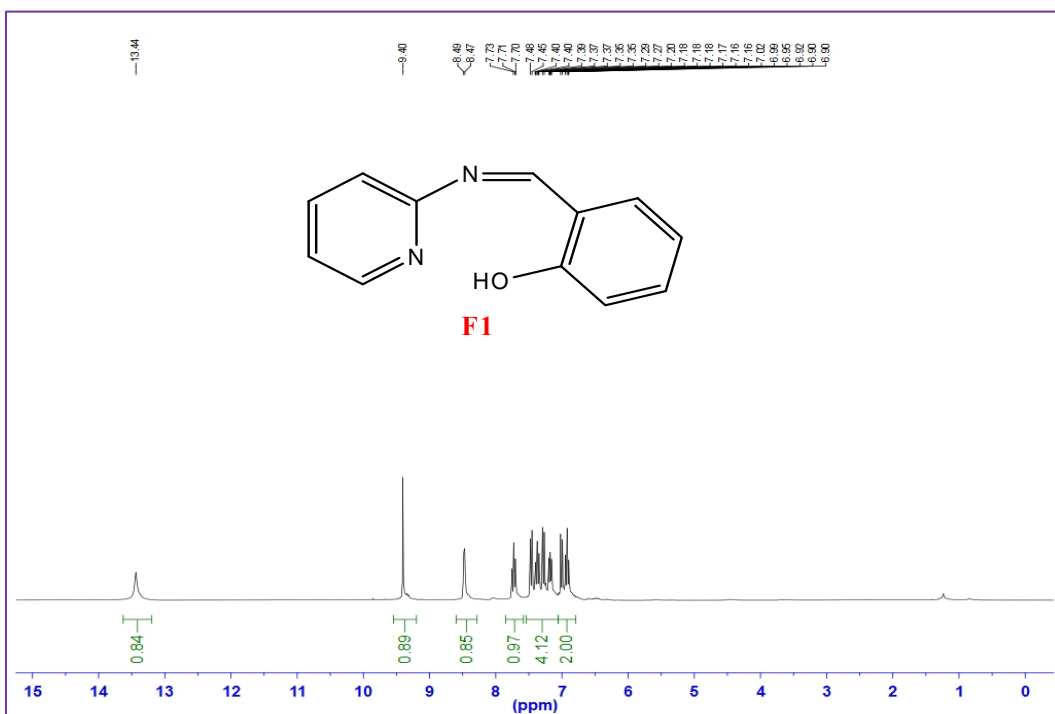


Figure S1 ¹H NMR spectrum of F1.

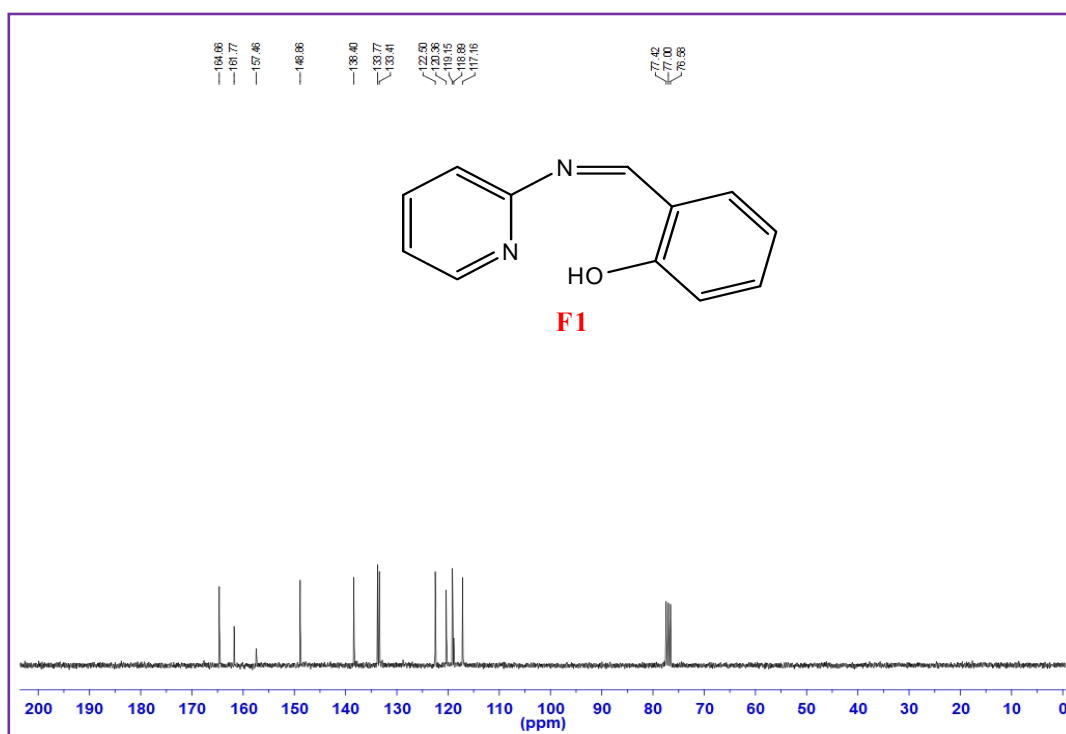


Figure S2 ¹³C NMR spectrum of F1.

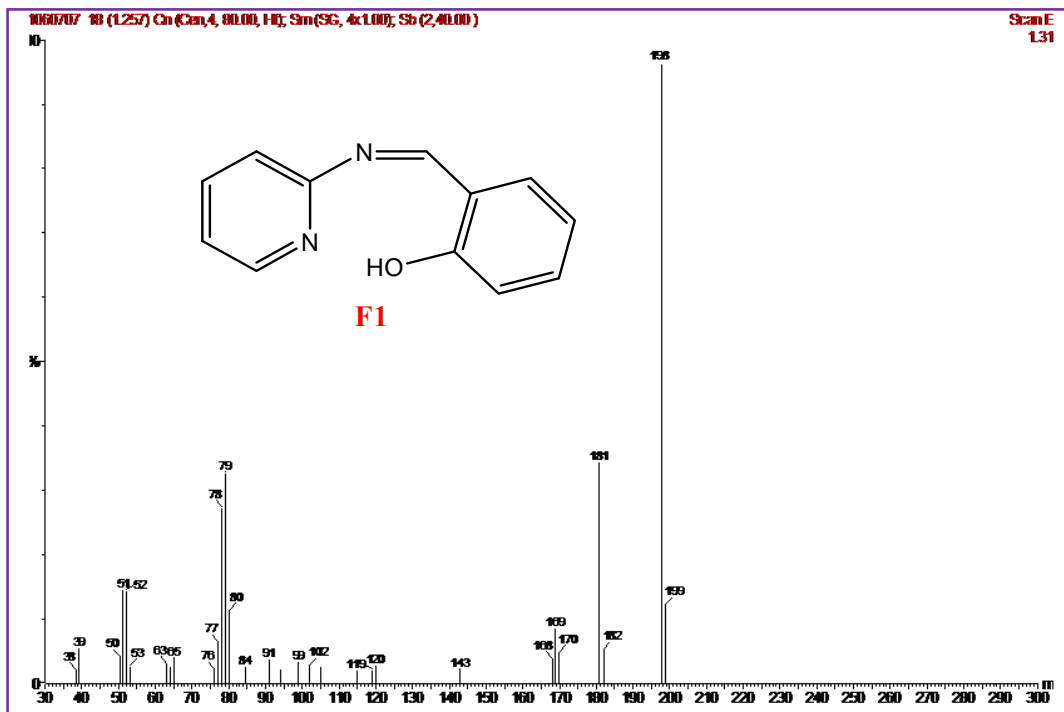


Fig. S3 Mass (FAB) spectrum of F1.

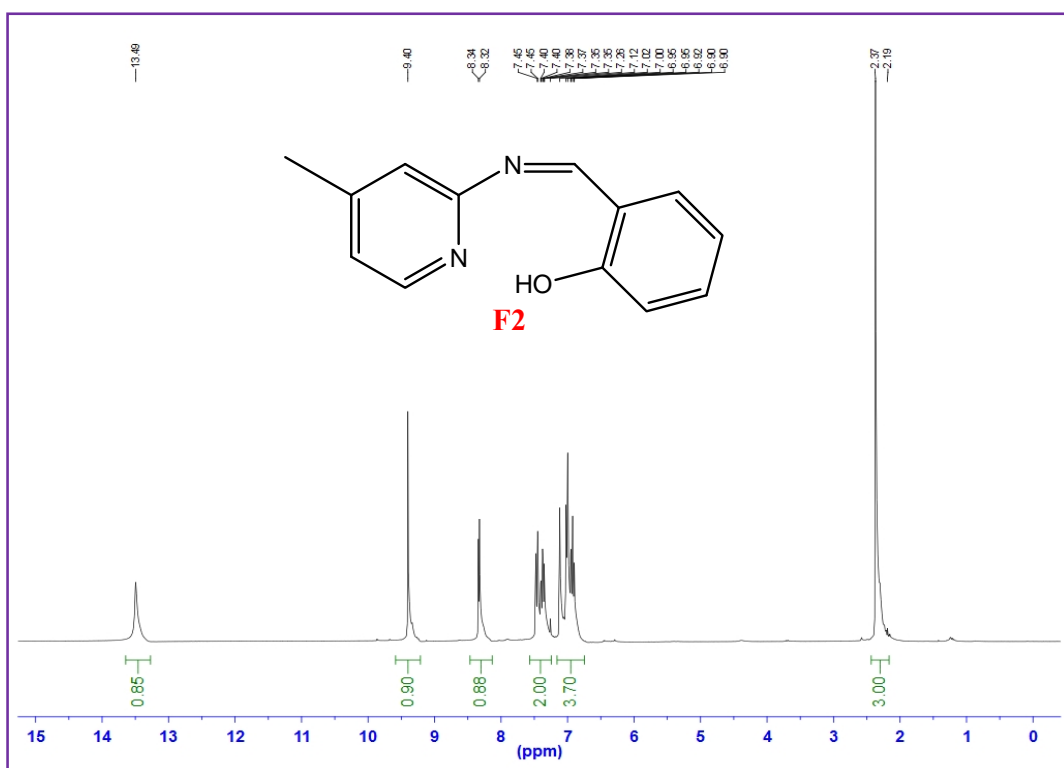


Fig. S4 ¹H NMR spectrum of F2.

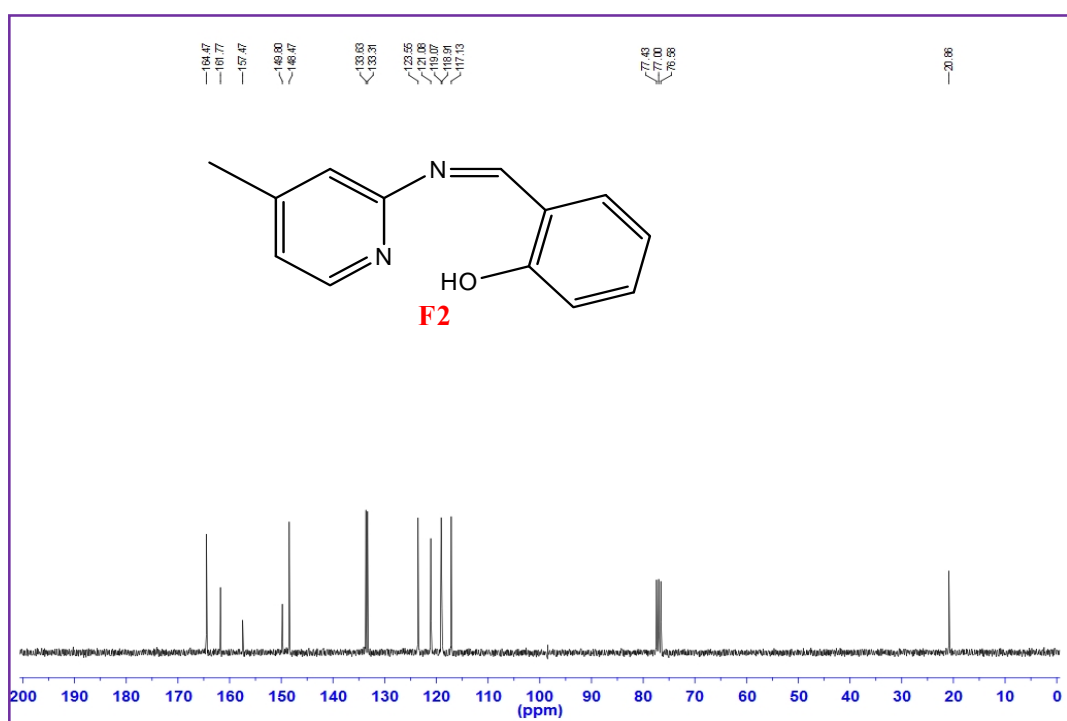


Fig. S5 ^{13}C NMR spectrum of F2.

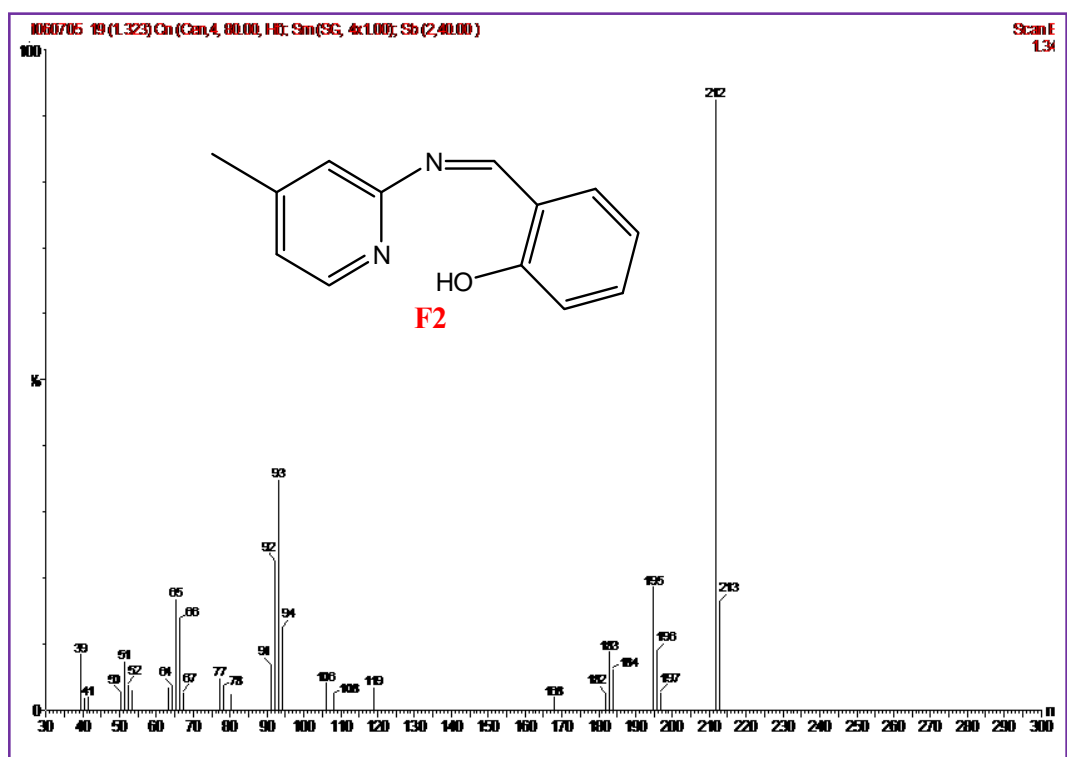


Fig. S6 Mass (FAB) spectrum of F2.

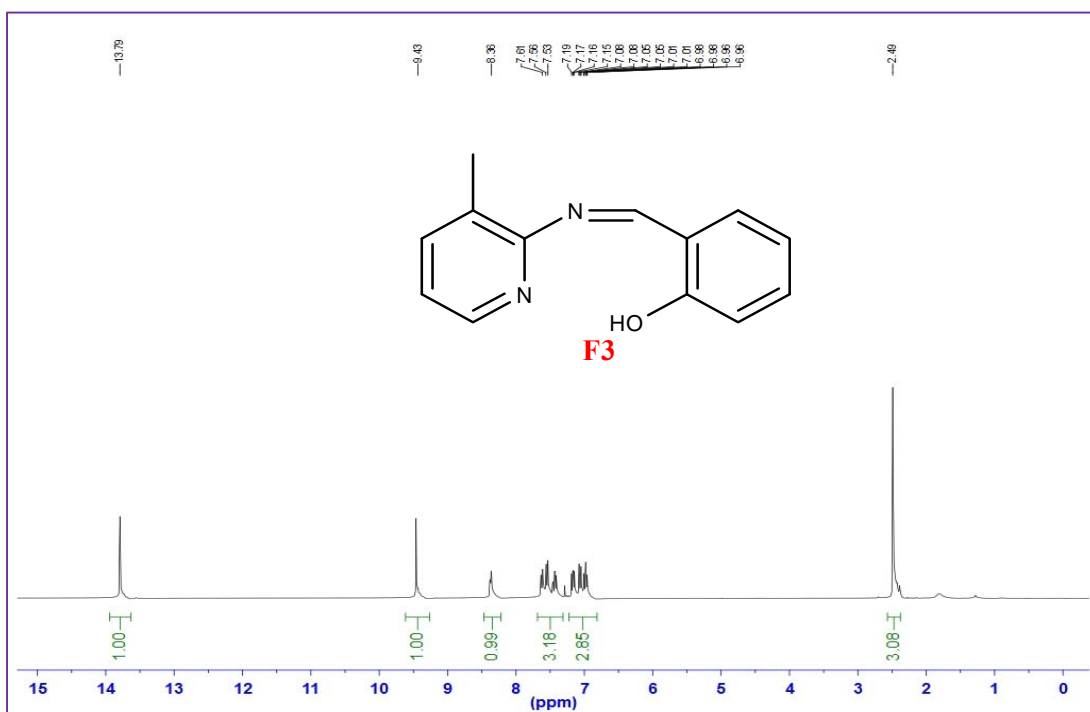


Fig. S7 ¹H NMR spectrum of F3.

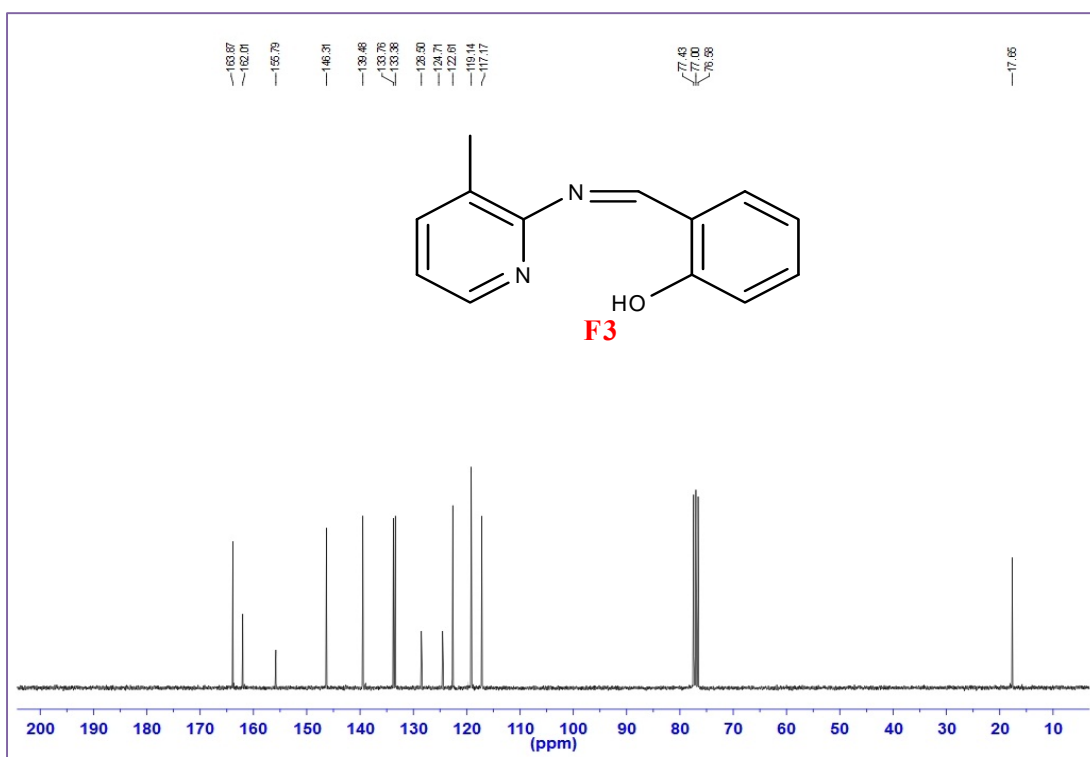


Fig. S8 ¹³C NMR spectrum of F3.

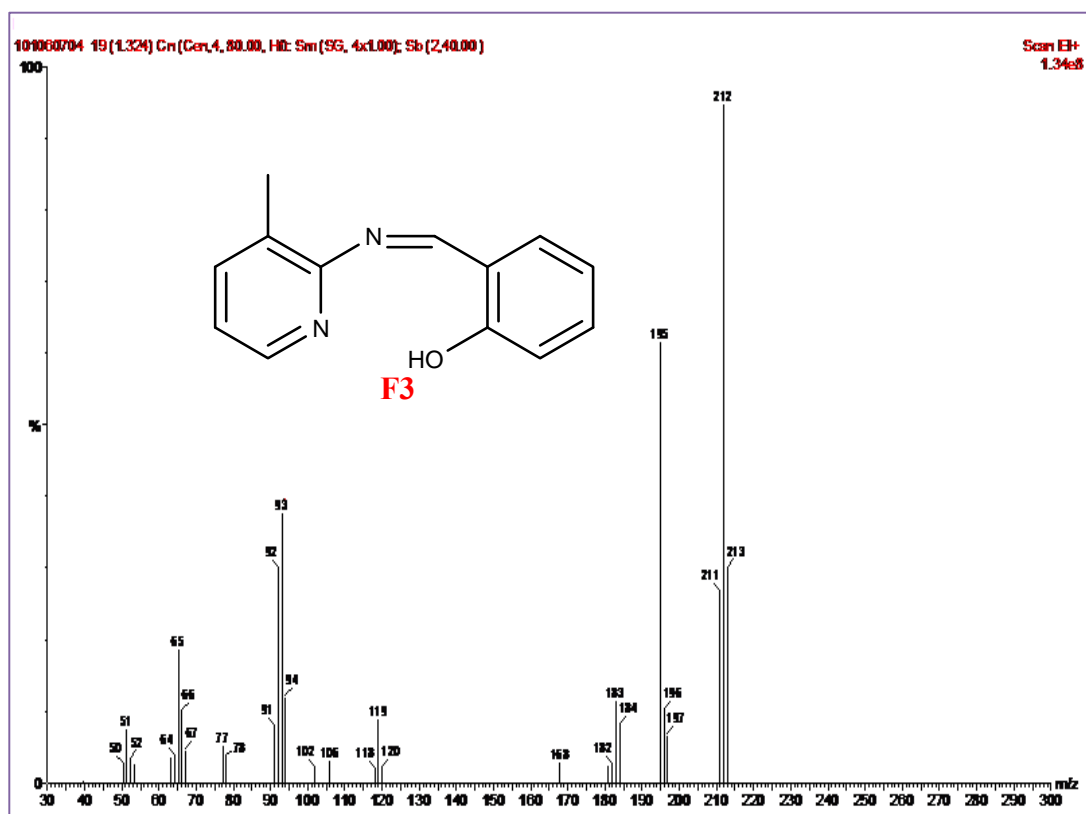


Fig. S9 Mass (FAB) spectrum of F3.

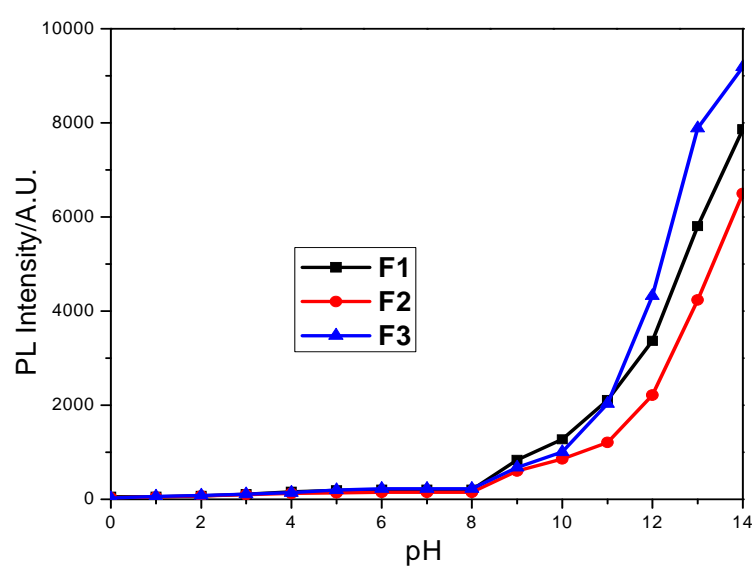


Fig. S10 PL spectral responses of (a) F1, (b) F2, and (c) F3 as function of pHs (0-14).

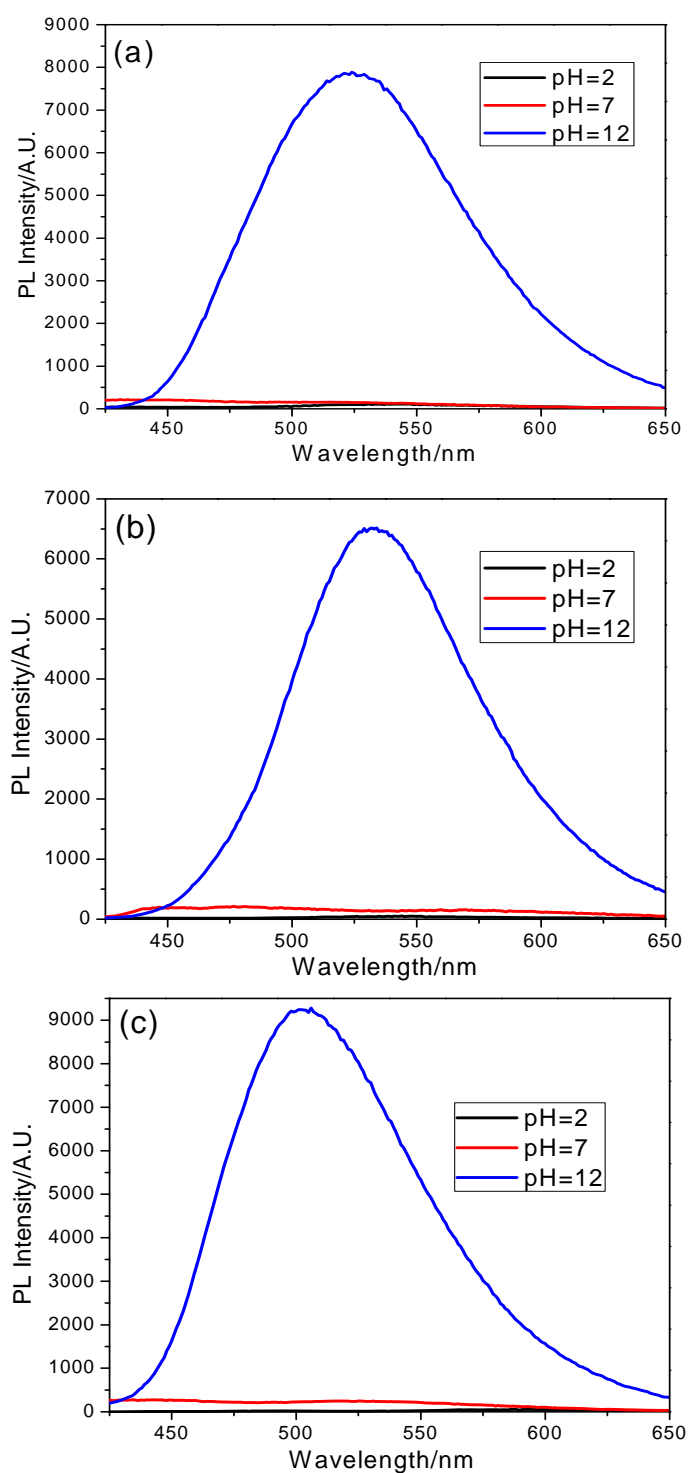


Fig. S11 PL spectra of **F1**, **F2** and **F3** (a, b, and c) at acidic, neutral, and basic pHs (2, 7, and 12).

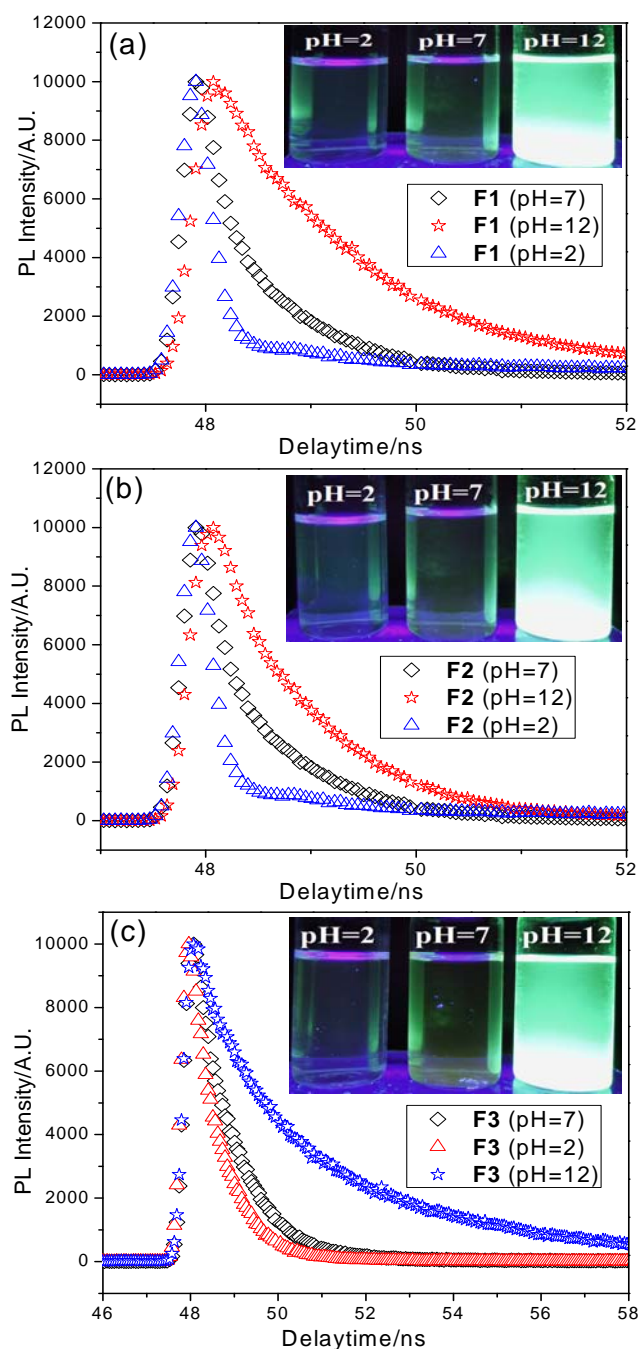


Fig. S12 Time-resolved fluorescence spectra of F1, F2 and F3 (a, b, and c) at acidic, neutral, and basic pHs (2, 7, and 12); Inset: Photographs of F1, F2 and F3 at acidic, neutral, and basic pHs (2, 7, and 12).

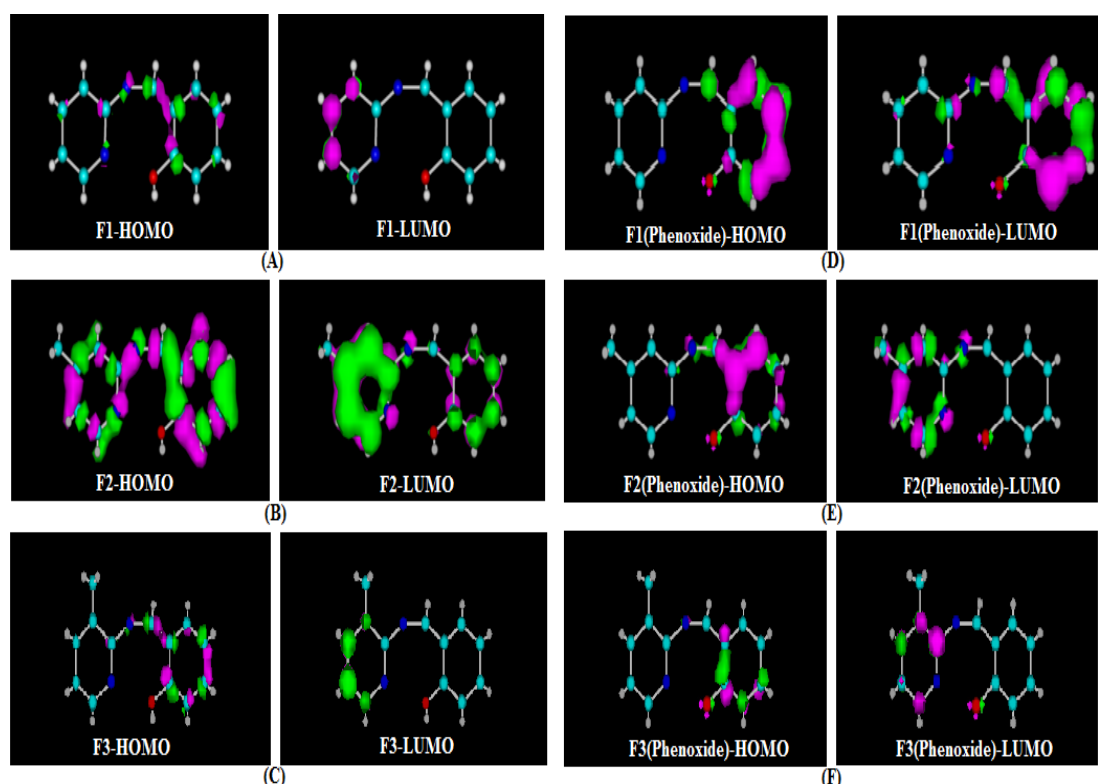


Fig. S13 Computational analysis of HOMO and LUMO levels of **F1**, **F2**, **F3**, **F1**-phenoxide, **F2**-phenoxide, and **F3**-phenoxide ions. (Semi-empirical AM1 method).

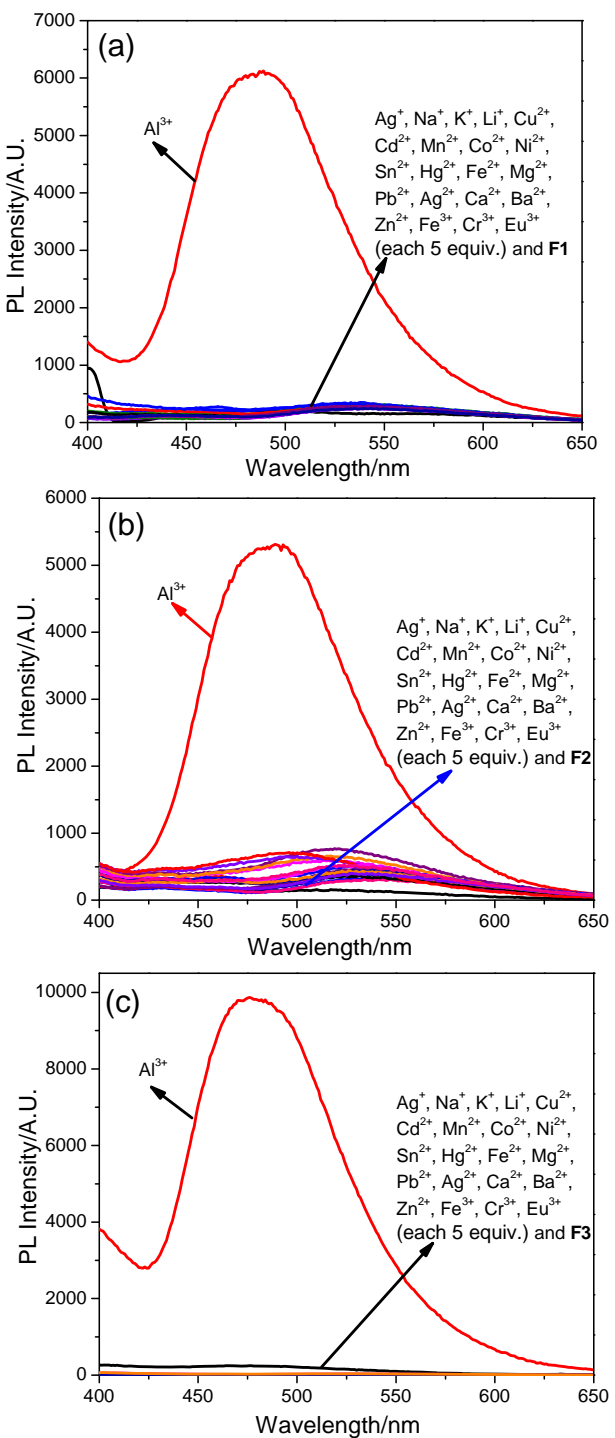


Fig. S14 Sensor responses of (a) **F1** in $\text{CH}_3\text{CN}/\text{H}_2\text{O}$ (3/7; vol/vol), (b) **F2** in $\text{CH}_3\text{CN}/\text{H}_2\text{O}$ (3/7; vol/vol), and (c) **F3** in $\text{CH}_3\text{CN}/\text{H}_2\text{O}$ (3/7; vol/vol) towards metal ions in H_2O .

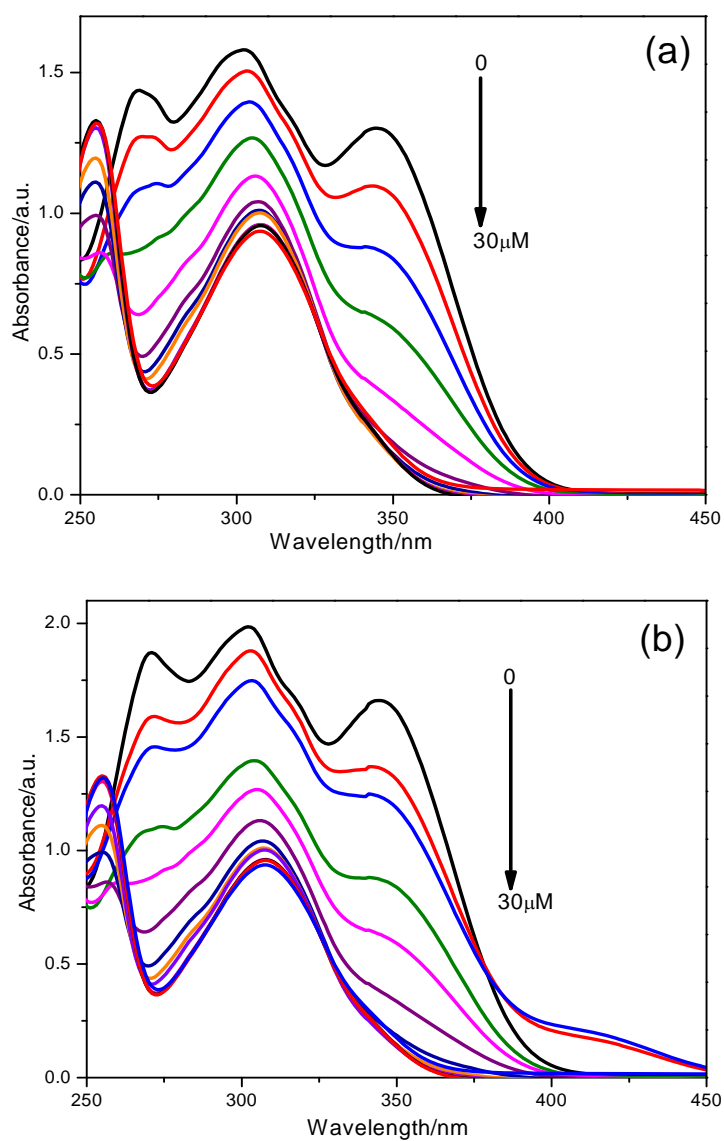


Fig. S15 UV-Vis titrations of (a) **F1** (20 μM), and (b) **F2** (20 μM) in CH₃CN/H₂O (6/4; vol/vol) upon the addition of Zn²⁺ (0, 5, 10, 15, 20, 22, 24, 28 and 30 μM).

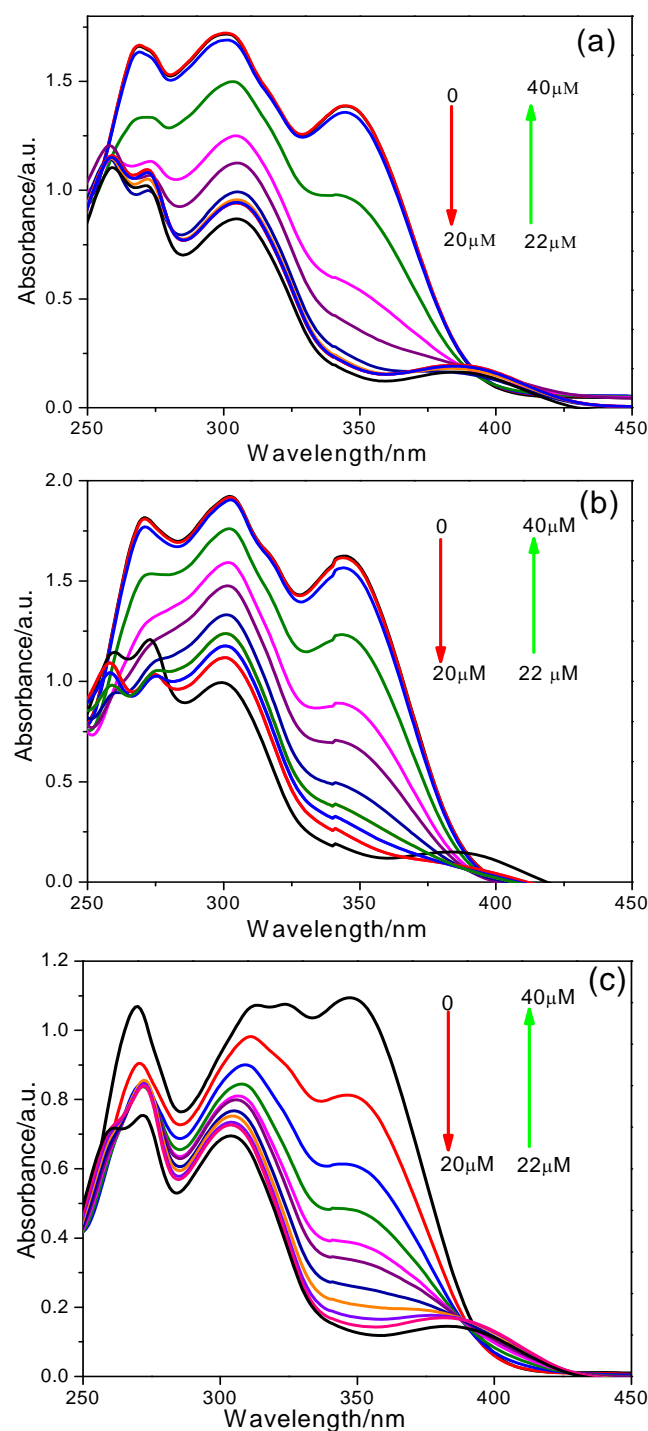


Fig. S16 UV-Vis titrations of (a) **F1** (20 μM), (b) **F2** (20 μM), and (c) **F3** (20 μM) in CH₃CN/H₂O (6/4 and 3/7; vol/vol ratios) upon the addition of Al³⁺ (0, 2, 5, 10, 15, 20, 22, 24, 28, 32, 36 and 40 μM).

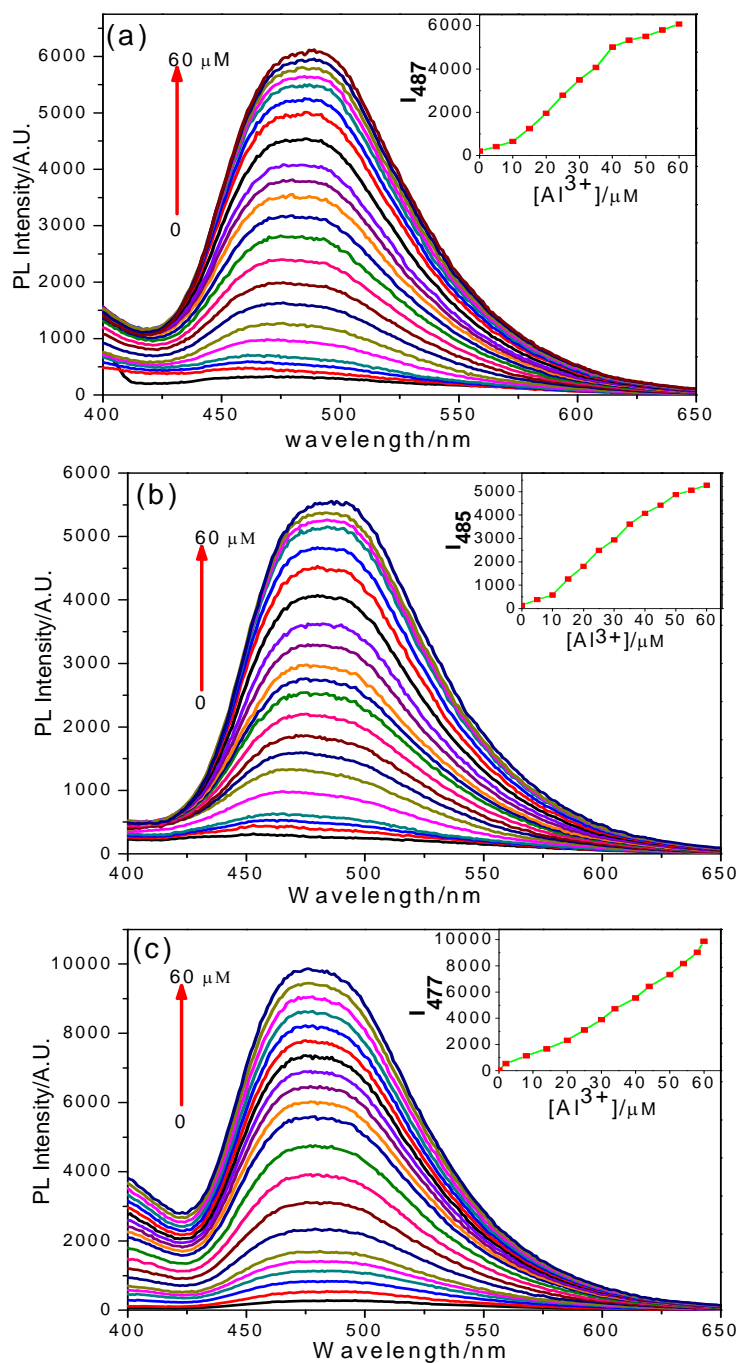


Fig. S17 Fluorescence spectral changes of (a) **F1** ($1 \times 10^{-5} M$) in CH_3CN/H_2O (3/7; vol/vol) ($\lambda_{ex}=344 nm$), (b) **F2** ($1 \times 10^{-5} M$) in CH_3CN/H_2O (3/7; vol/vol) ($\lambda_{ex}=346 nm$), and (c) **F3** ($1 \times 10^{-5} M$) in CH_3CN/H_2O (3/7; vol/vol) ($\lambda_{ex}=343 nm$) titrated with 0-60 μM of Al^{3+} ions in H_2O (with an equal span of 3 μM). Insets show PL spectral responses of (a) **F1**, (b) **F2** and (c) **F3** as a function of Al^{3+} .

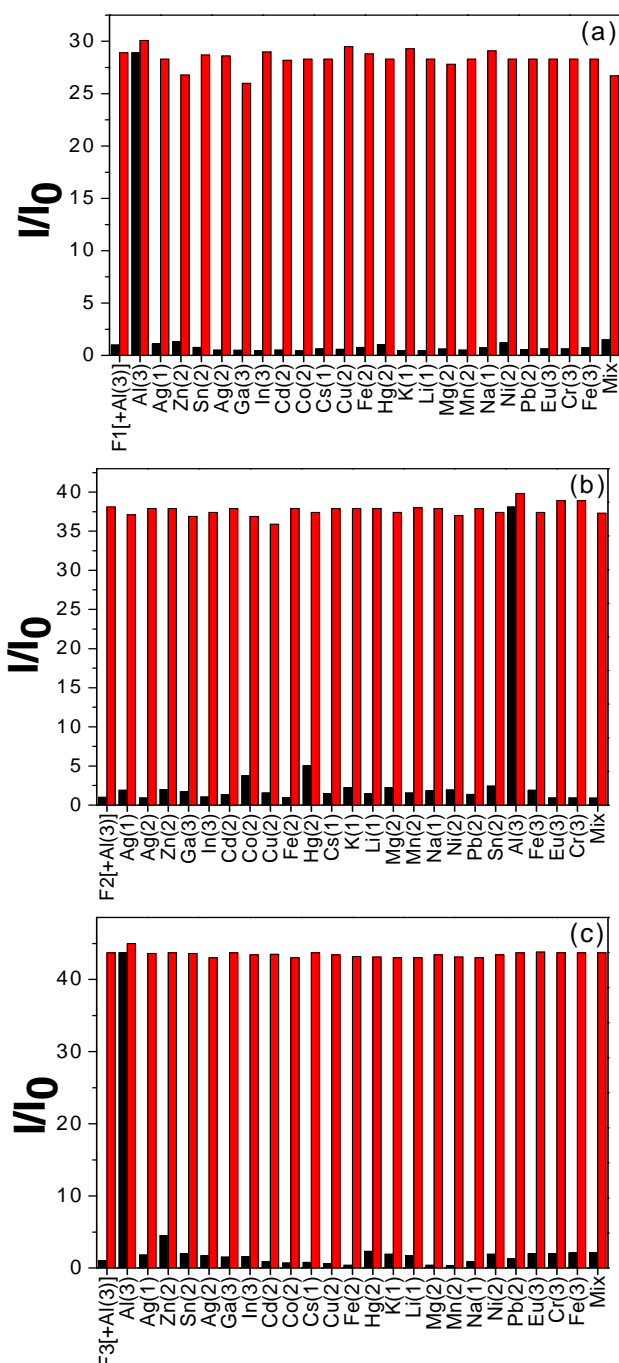


Fig. S18 Relative fluorescence intensities of (a) **F1** (20 μM), (b) **F2** (20 μM) and (c) **F2** (20 μM) in $\text{CH}_3\text{CN}/\text{H}_2\text{O}$ (3/7; vol/vol) with 60 μM Al^{3+} in H_2O in the presence of competing metal ions. Black bars; **F1**, **F2**, and **F3** (20 μM) in $\text{CH}_3\text{CN}/\text{H}_2\text{O}$ (3/7; vol/vol) with 60 μM of stated metal ions in H_2O . Red bars; **F1**, **F2**, and **F3** (20 μM) $\text{CH}_3\text{CN}/\text{H}_2\text{O}$ (3/7; vol/vol) with 60 μM Al^{3+} + 60 μM of stated metal ions in H_2O . (120 μM of Al^{3+} for Al^{3+} effect). (Mix = all metal ions except Zn^{2+} and Al^{3+}).

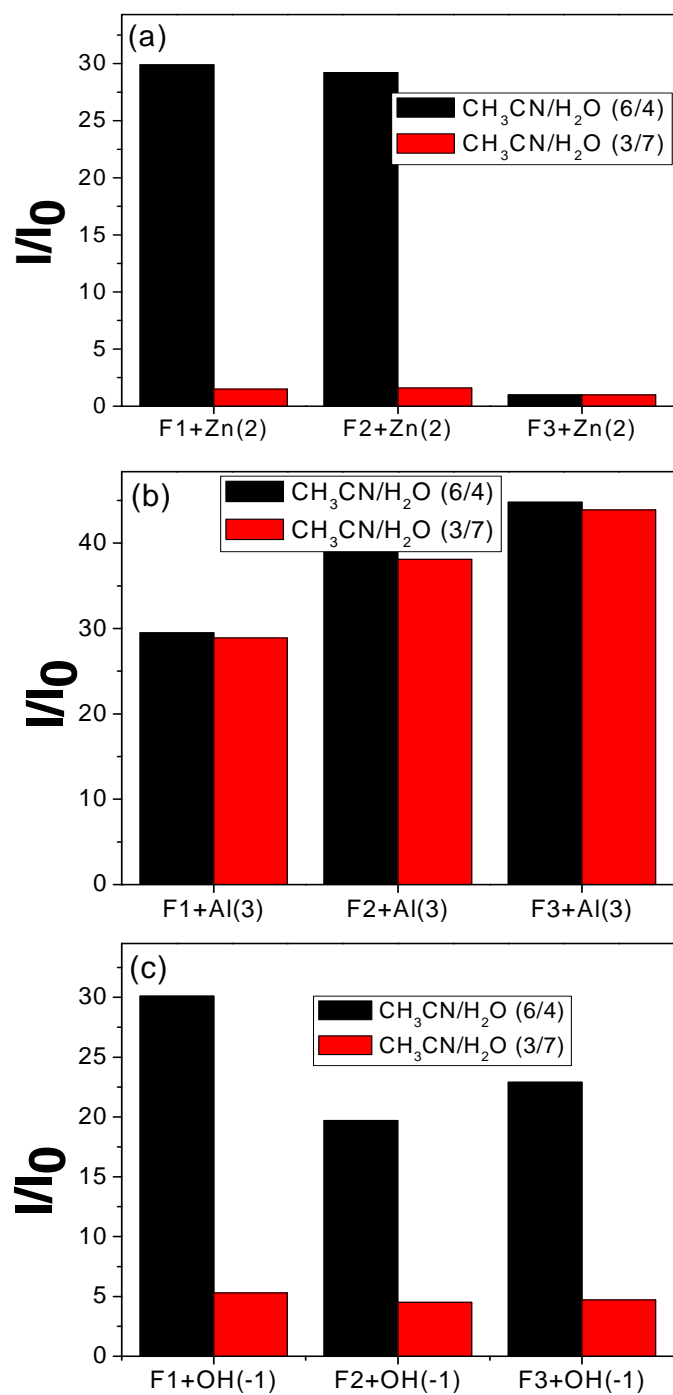


Fig. S19 Comparison of relative fluorescence intensity changes of (a) **F1** in $\text{CH}_3\text{CN}/\text{H}_2\text{O}$ (6/4 and 3/7; vol/vol ratios), (b) **F2** in $\text{CH}_3\text{CN}/\text{H}_2\text{O}$ (6/4 and 3/7; vol/vol ratios), and (c) **F3** in $\text{CH}_3\text{CN}/\text{H}_2\text{O}$ (6/4 and 3/7; vol/vol ratios) towards Zn^{2+} , Al^{3+} and OH^- ions in H_2O .

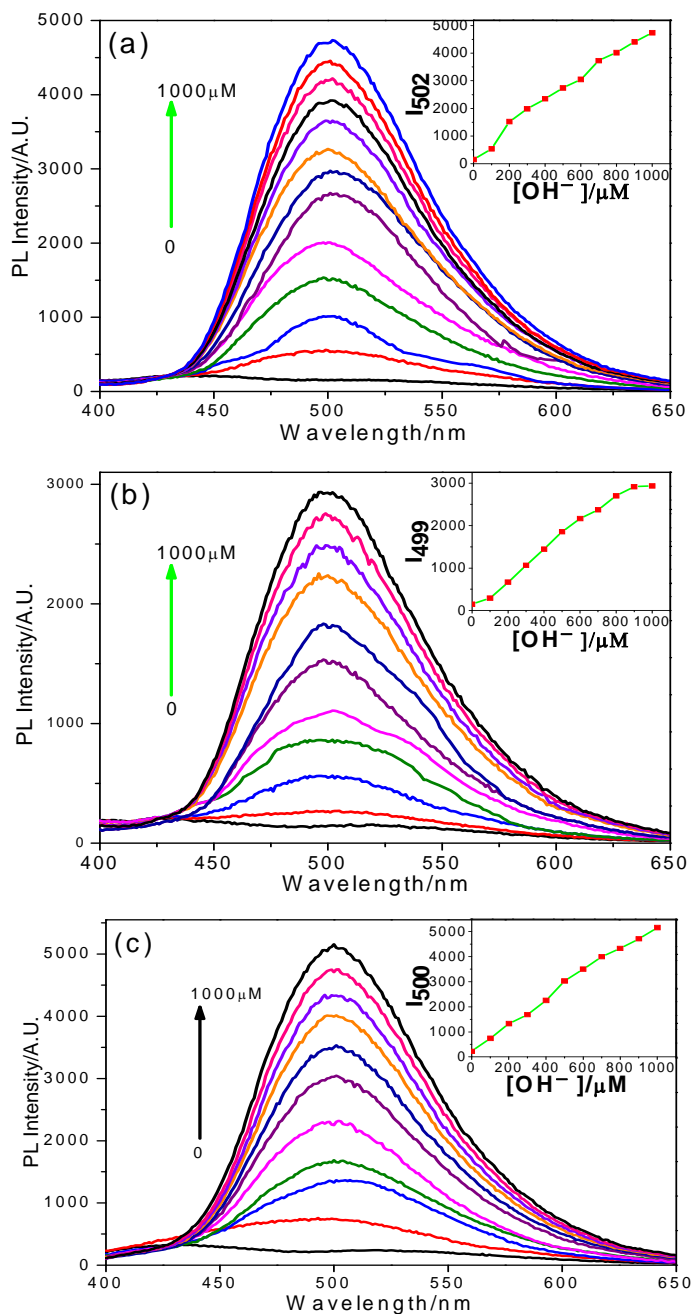


Fig. S20 Fluorescence spectral changes of (a) **F1** (20 μM) in CH₃CN/H₂O (6/4; vol/vol) ($\lambda_{\text{ex}}=346$ nm), (b) **F2** (20 μM) in CH₃CN/H₂O (6/4; vol/vol) ($\lambda_{\text{ex}}=344$ nm) and (c) **F3** (20 μM) in CH₃CN/H₂O (6/4; vol/vol) ($\lambda_{\text{ex}}=343$ nm) titrated with 0–1000 μM of OH⁻ ion in H₂O (0, 100, 200, 300, 400, 500, 600, 700, 800, 850, 900, 950 and 1000 μM) were plotted for **F1**, and **F2** was plotted with an equal span of 100 μM. Insets showed PL spectral responses of (a) **F1** and (b) **F2** as a function of OH⁻ ion.

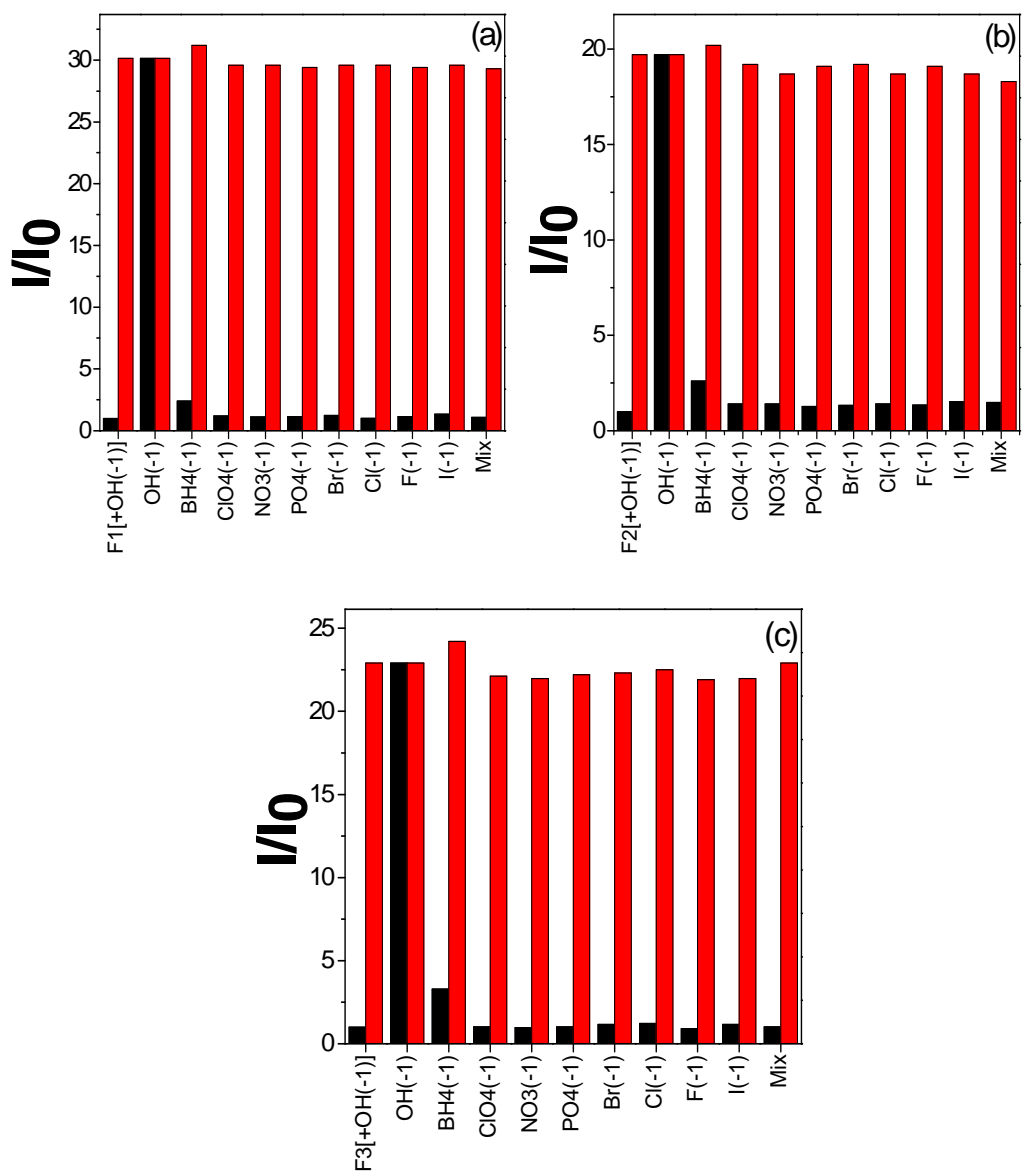


Fig. S21 Relative fluorescence intensities of (a) **F1** (20 μM), (b) **F2** (20 μM), and (c) **F3** (20 μM) in $\text{CH}_3\text{CN}/\text{H}_2\text{O}$ (6/4; vol/vol) with 1000 μM OH⁻ in H_2O in the presence of competing anions. Black bars; **F1** or **F2** (20 μM) in $\text{CH}_3\text{CN}/\text{H}_2\text{O}$ (6/4; vol/vol) with 1000 μM of stated anions in H_2O . Red bars; **F1** or **F2** (20 μM) $\text{CH}_3\text{CN}/\text{H}_2\text{O}$ (6/4; vol/vol) with 1000 μM OH⁻ + 1000 μM of stated anions in H_2O . (for OH⁻ effect 2000 μM of OH⁻). (Mix = all anions except OH⁻).

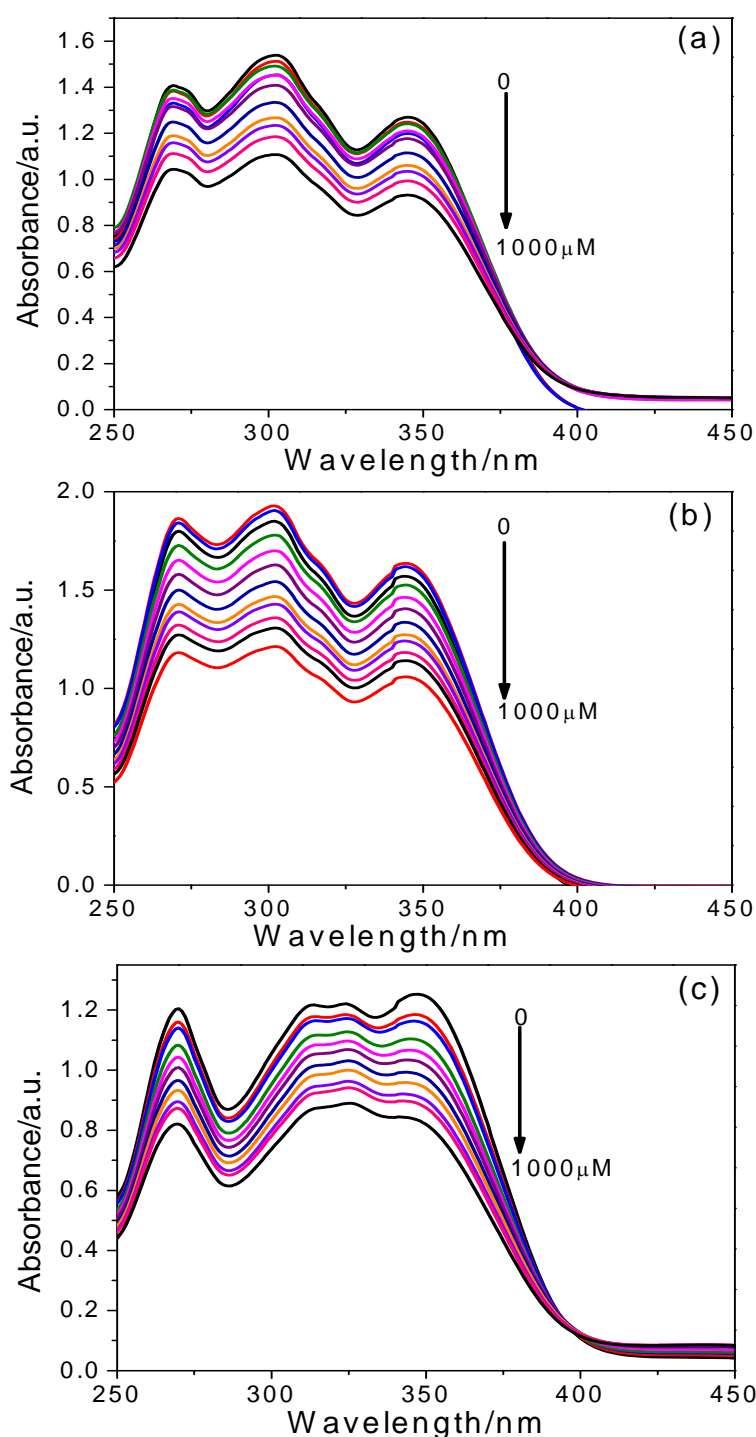


Fig. S22 UV-Vis absorption spectral changes of (a) **F1** (b) **F2**, and (c) **F3**, upon the addition of OH⁻ ions (0-1000 μM with an equal span of 100 μM).

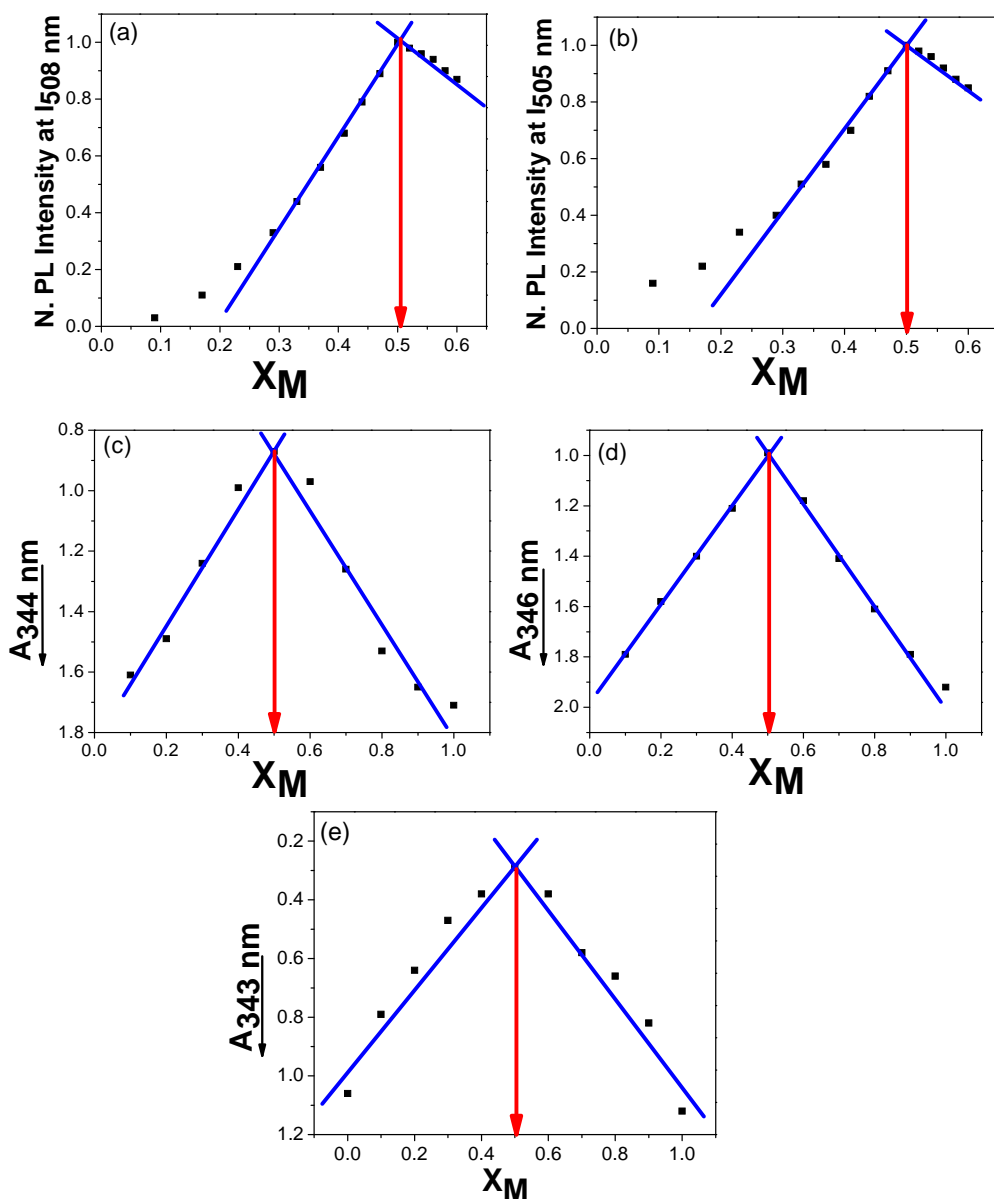


Fig. S23 Job plots for determination of stoichiometries of (a) **F1** + Zn^{2+} , (b) **F2** + Zn^{2+} , (c) **F1** + Al^{3+} , (d) **F2** + Al^{3+} , and (e) **F3** + Al^{3+} ; $X_M = [M^{n+}] / [M^{n+}] + [F1 \text{ or } F2 \text{ or } F3]$; for (a), (b) $[M^{n+}] = Zn^{2+}$, and for (c), (d) and (e) $[M^{n+}] = Al^{3+}$. [Note: for (a), (b) stoichiometry calculations based on normalized PL spectral changes of **F1** and **F2** during the titration of Zn^{2+} , and for (c), (d) and (e) it was calculated from the UV-Vis spectral changes of Al^{3+} titrations with **F1**, **F2** and **F3**]

F1+ Zn^{2+} = 1:1 stoichiometry (ca. 0.506); **F1**+ Al^{3+} = 1:1 stoichiometry (ca. 0.500)

F2+ Zn^{2+} = 1:1 stoichiometry (ca. 0.503); **F2**+ Al^{3+} = 1:1 stoichiometry (ca. 0.507) and

F3+ Al^{3+} = 1:1 stoichiometry (ca. 0.508)

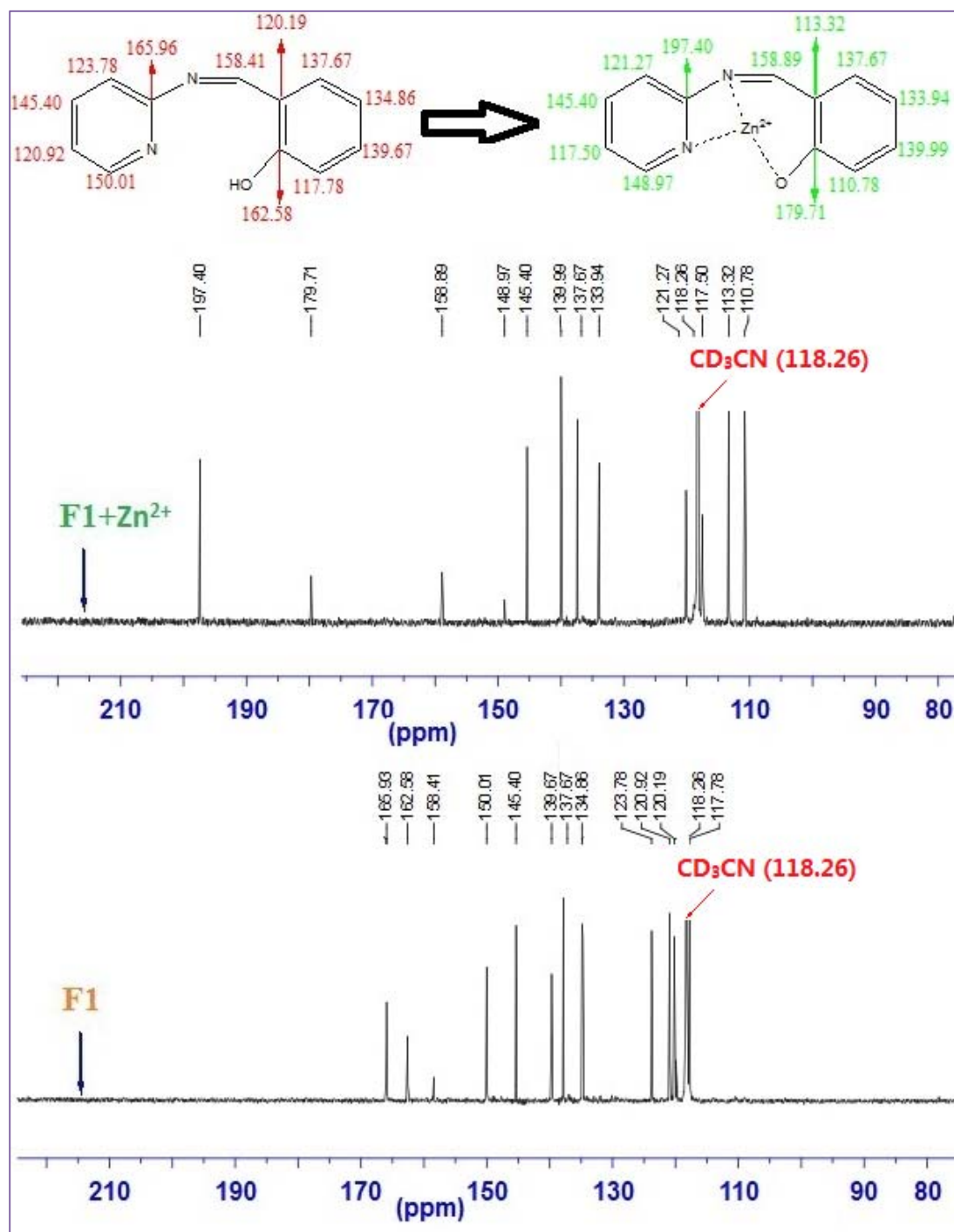


Fig. S24 ^{13}C NMR spectral changes of **F1** (1 equiv.) in CD_3CN with Zn^{2+} (1 equiv.) in D_2O .

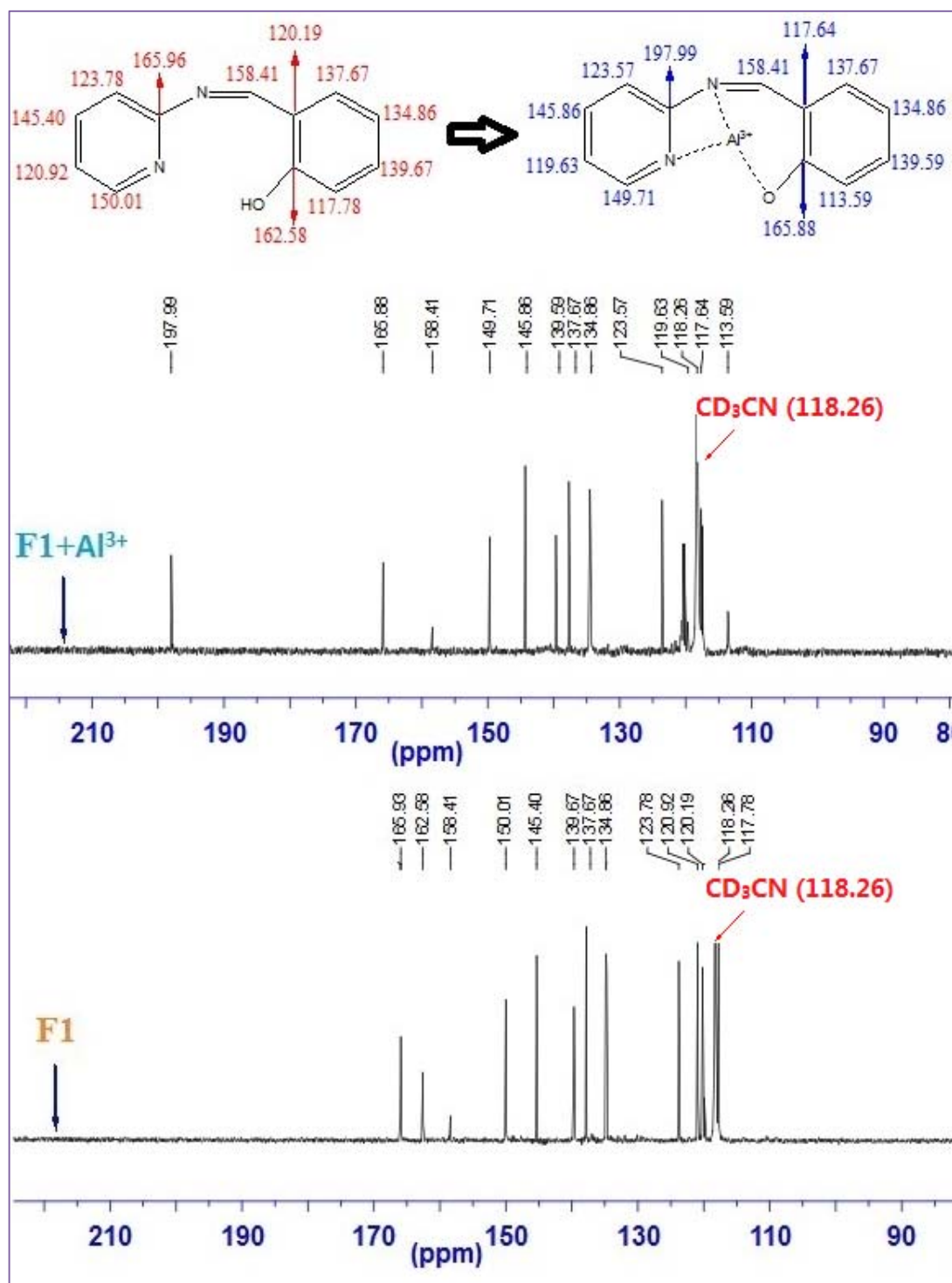


Fig. S25 ^{13}C NMR spectral changes of **F1** (1 equiv.) in CD_3CN with Al^{3+} (1 equiv.) in D_2O .

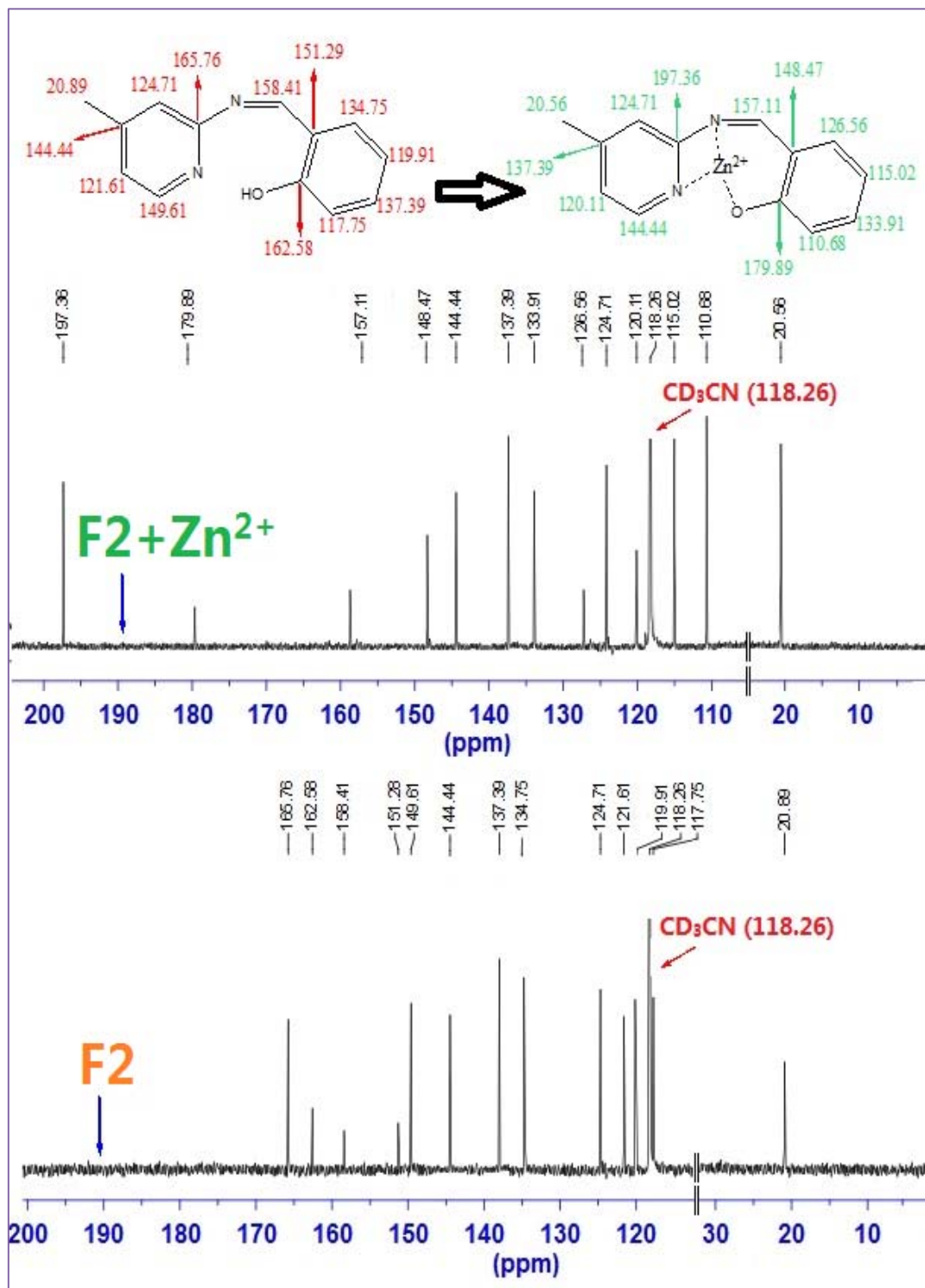


Fig. S26 ^{13}C NMR spectral changes of **F2** (1 equiv.) in CD_3CN with Zn^{2+} (1 equiv.) in D_2O .

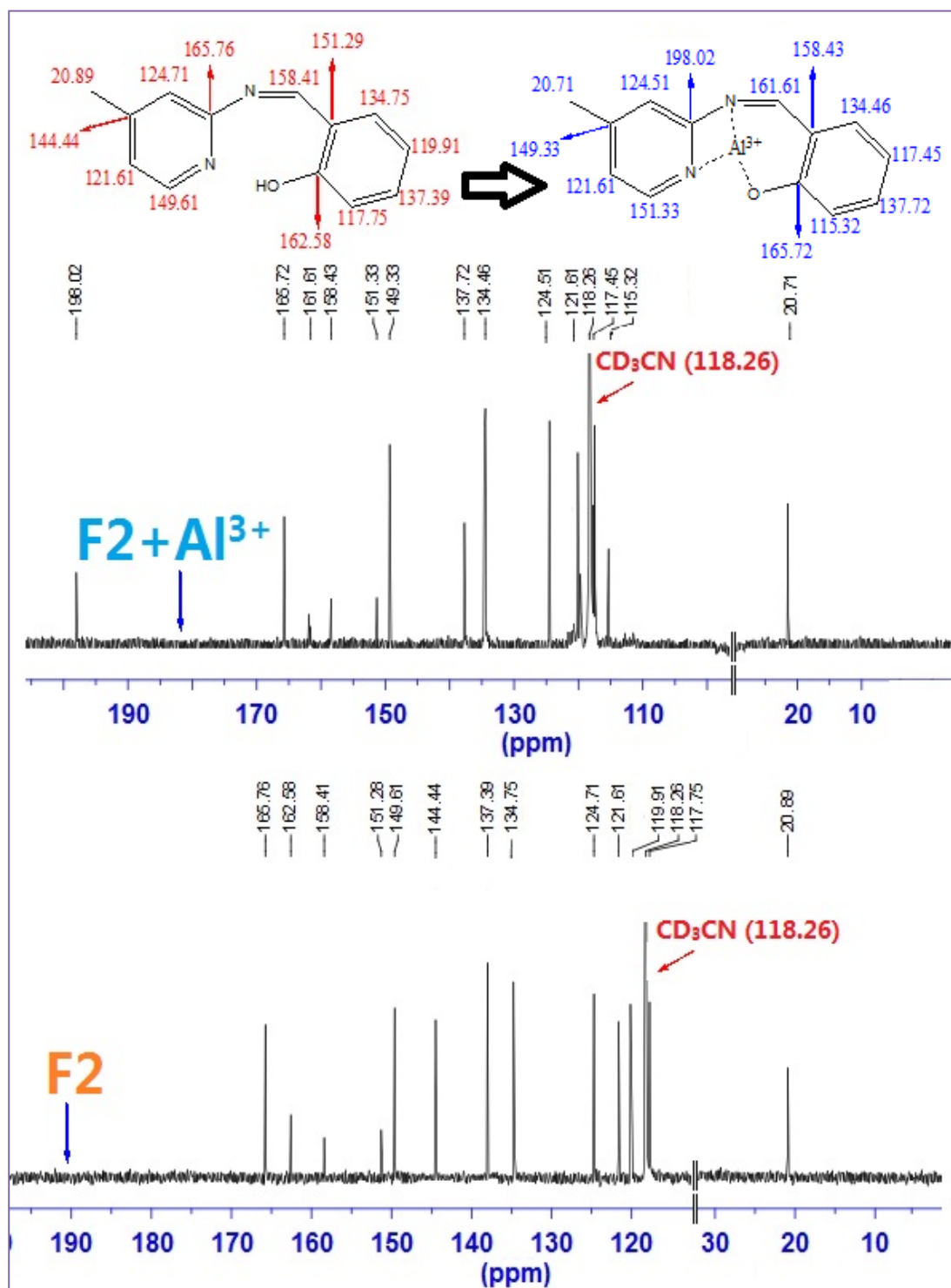


Fig. S27 ^{13}C NMR spectral changes of **F2** (1 equiv.) in CD_3CN with Al^{3+} (1 equiv.) in D_2O .

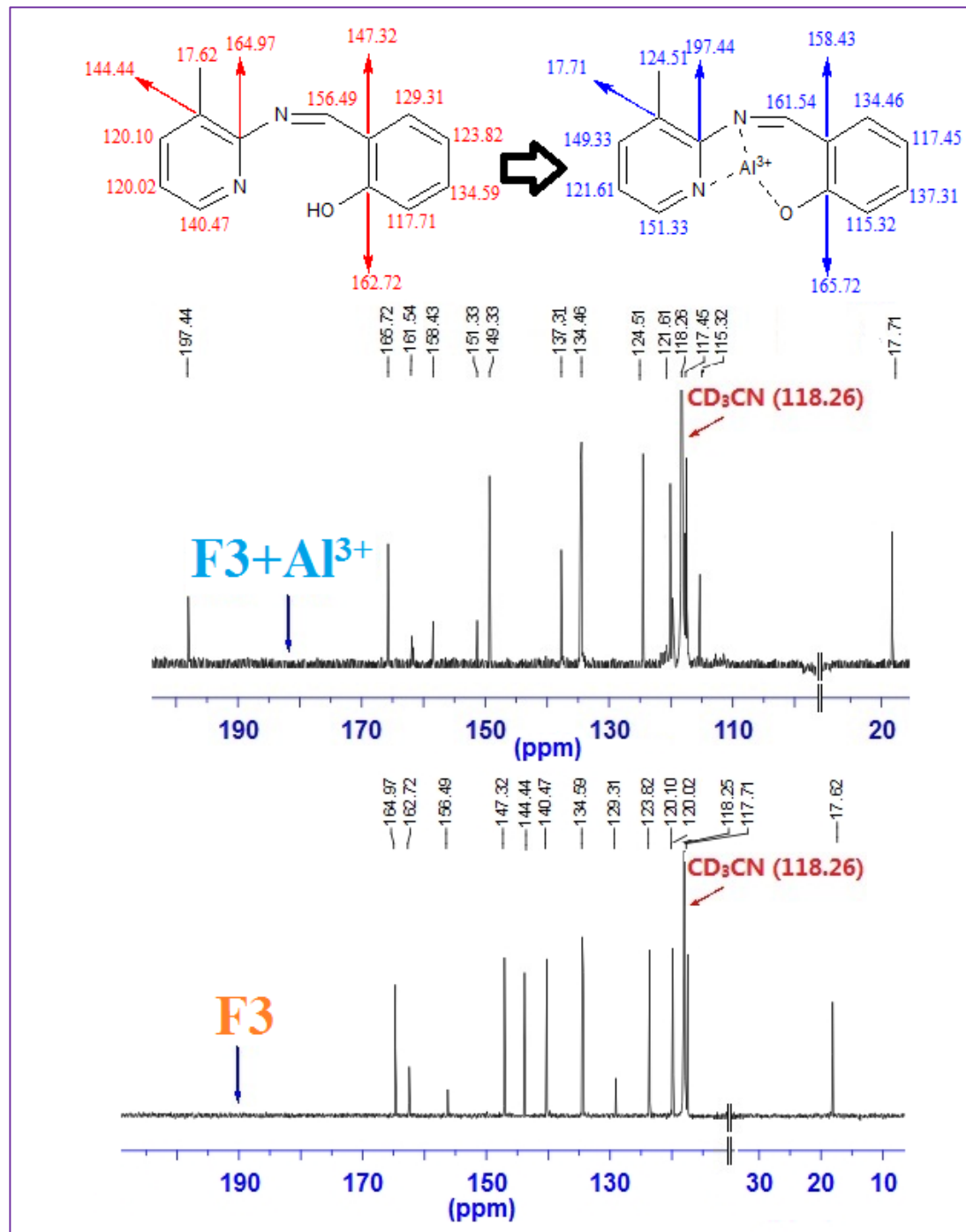


Fig. S28 ^{13}C NMR spectral changes of **F3** (1 equiv.) in CD_3CN with Al^{3+} (1 equiv.) in D_2O .

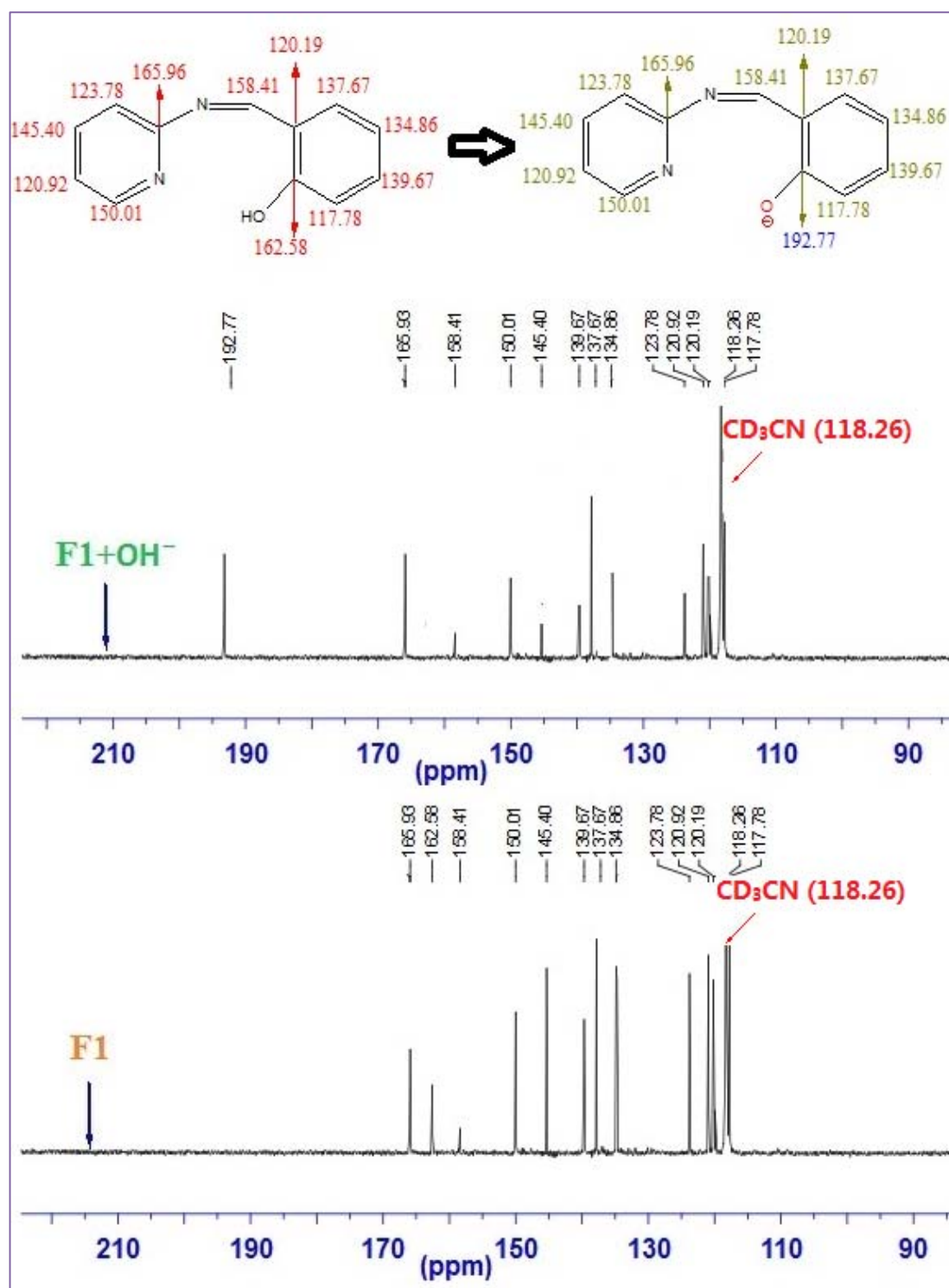


Fig. S29 ¹³C NMR spectral changes of **F1** (1 equiv.) in CD₃CN with OH⁻ (5 equiv.) in D₂O.

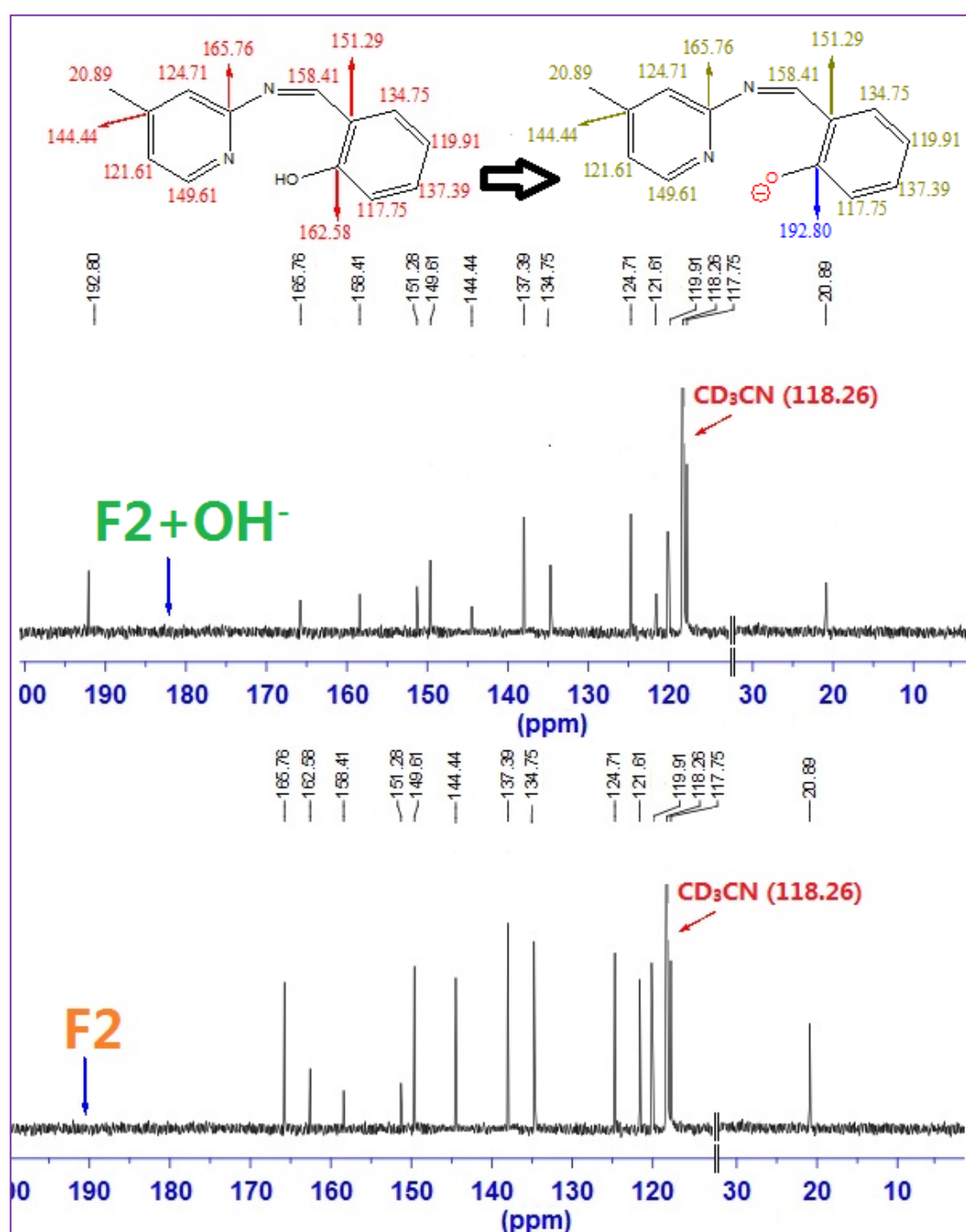


Fig. S30 ¹³C NMR spectral changes of F2 (1 equiv.) in CD₃CN with OH⁻ (5 equiv.) in D₂O.

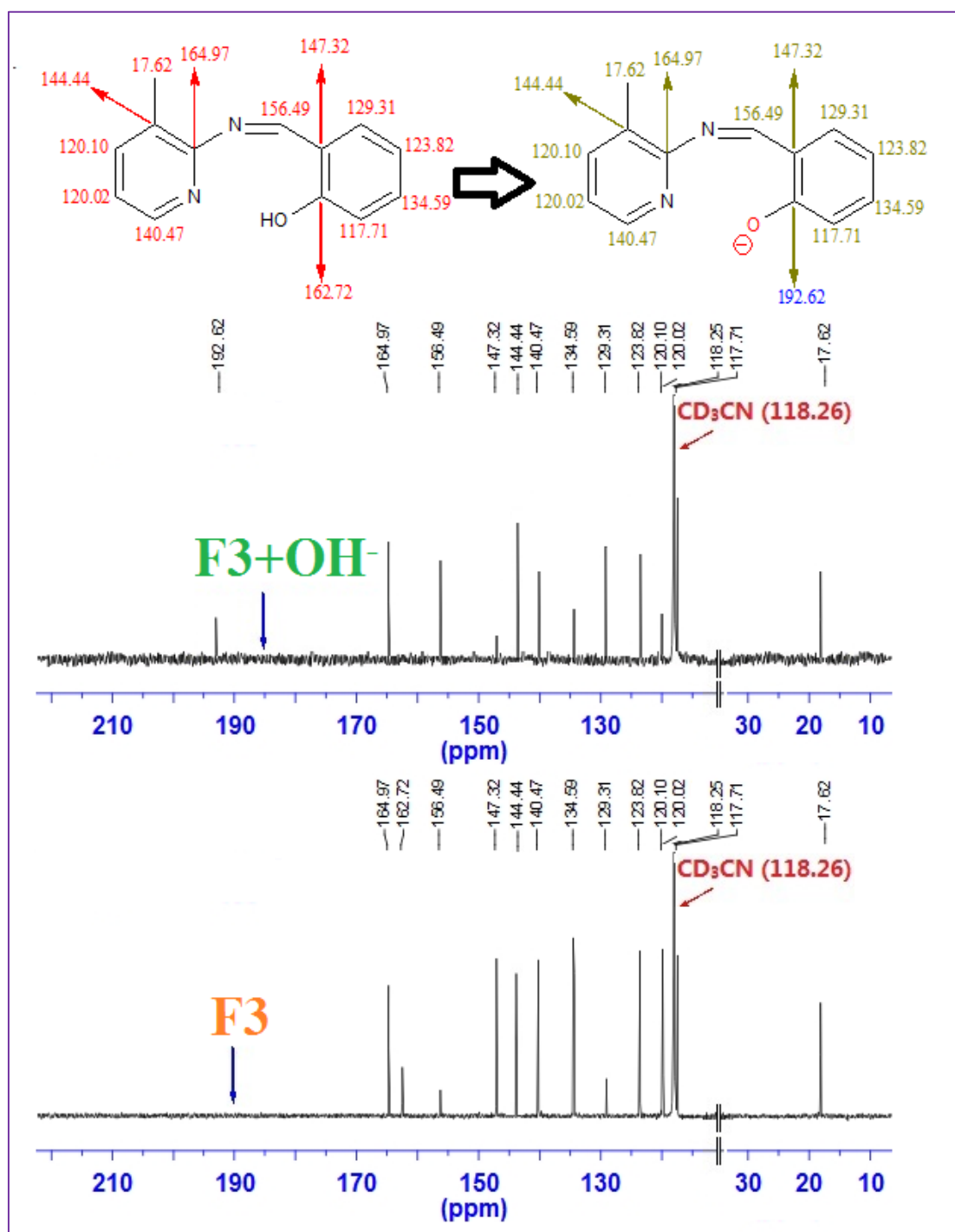


Fig. S31 ¹³C NMR spectral changes of F3 (1 equiv.) in CD₃CN with OH⁻ (5 equiv.) in D₂O.

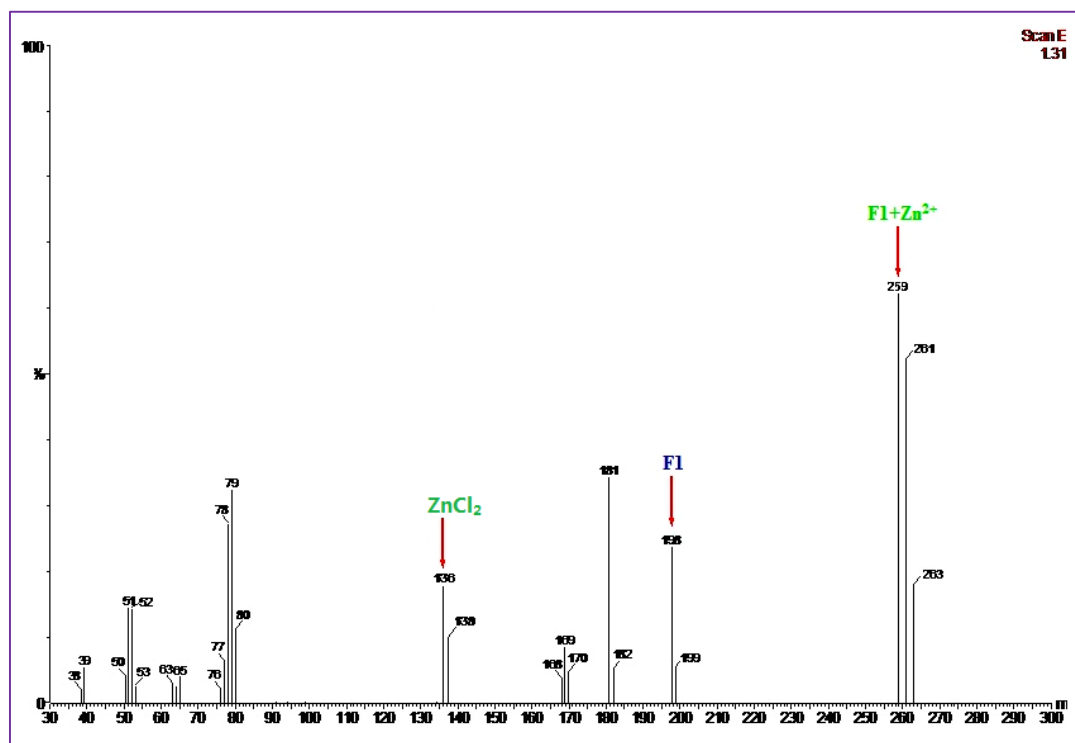


Fig. S32 Mass (FAB) spectral changes of **F1** (1 equiv.) + Zn²⁺ (1 equiv.).

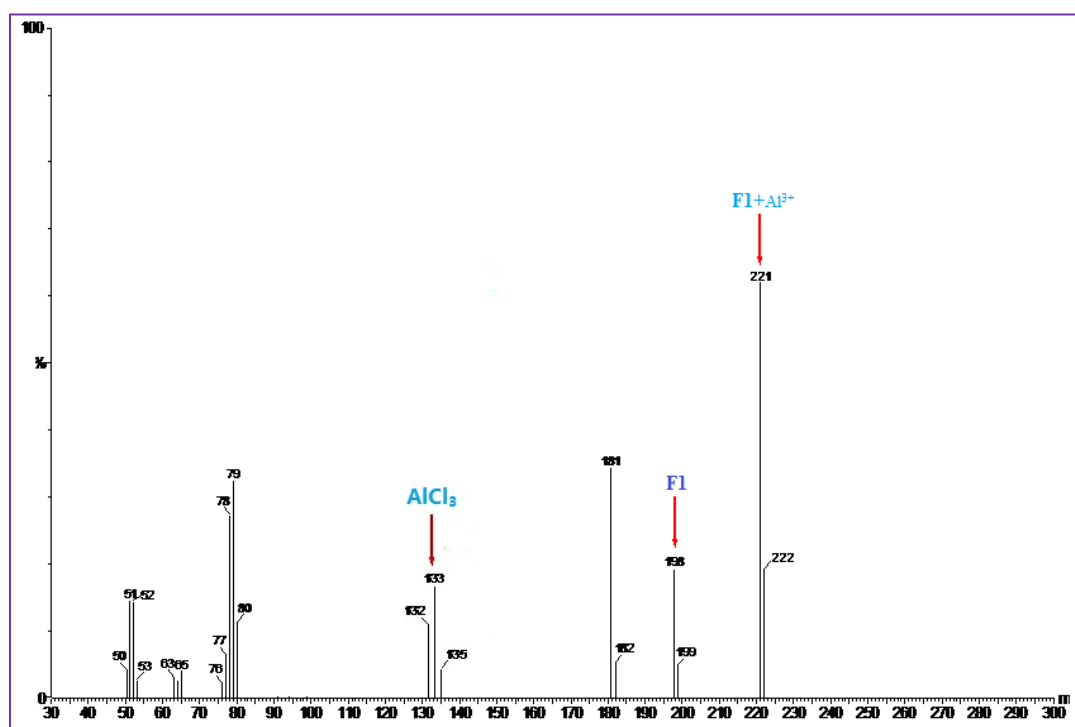


Fig. S33 Mass (FAB) spectral changes of **F1** (1 equiv.) + Al³⁺ (1 equiv.).

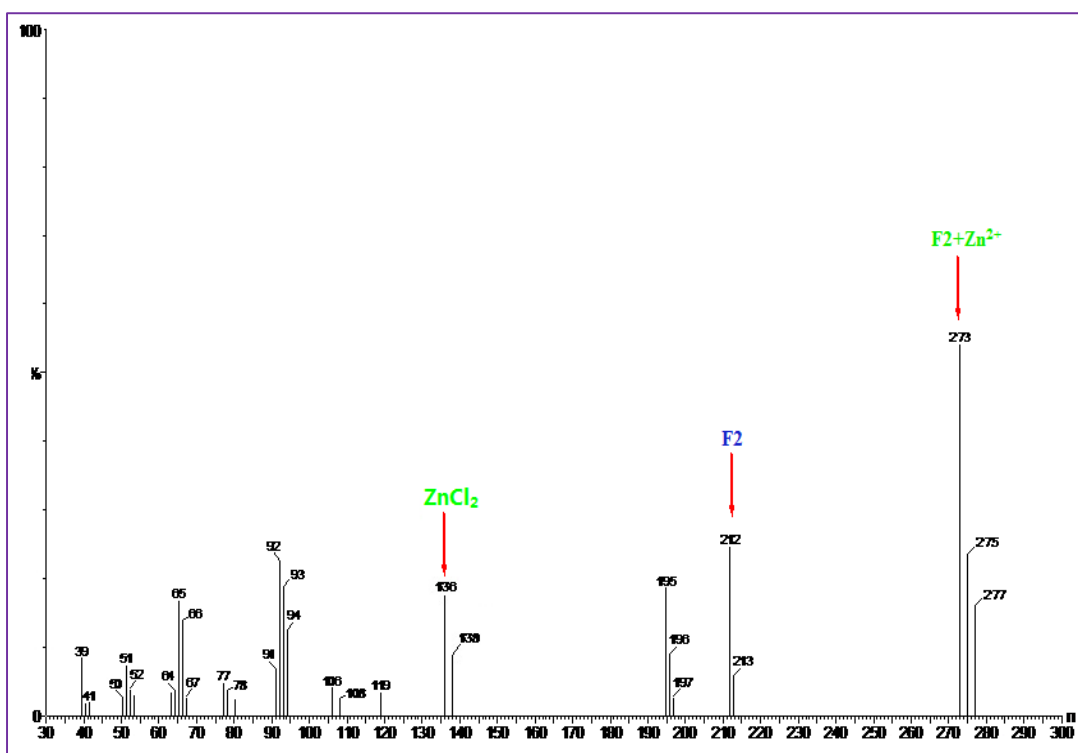


Fig. S34. Mass (FAB) spectral changes of **F2** (1 equiv.) + Zn²⁺ (1 equiv.).

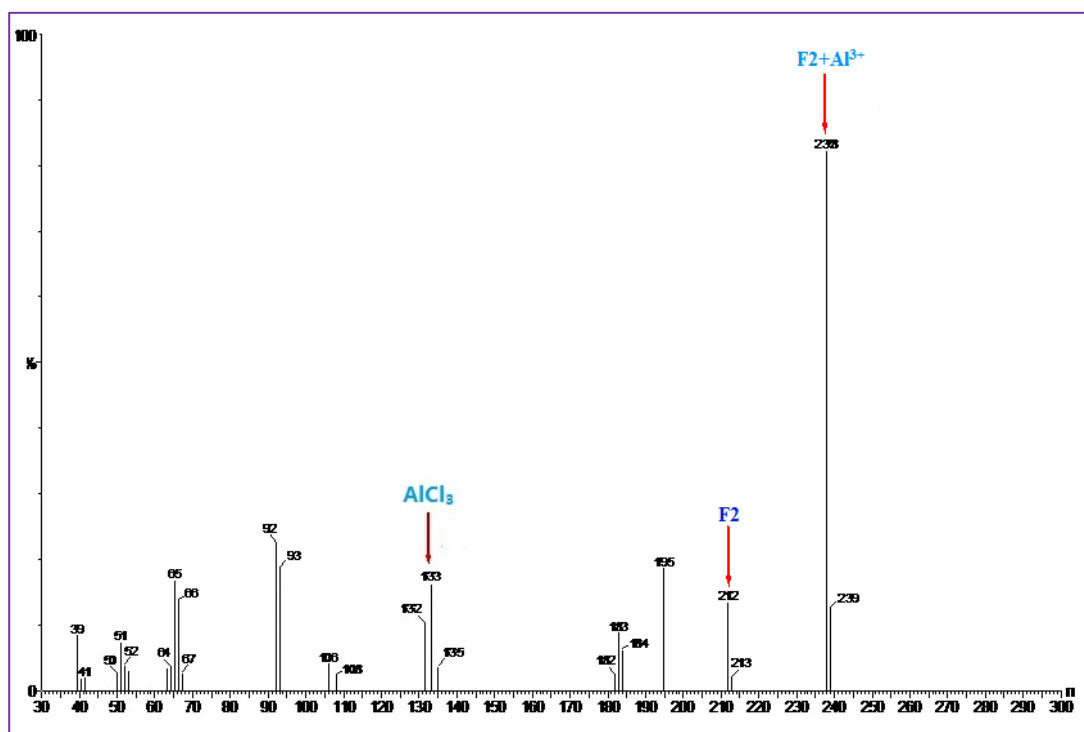


Fig. S35 Mass (FAB) spectral changes of **F2** (1 equiv.) + Al³⁺ (1 equiv.).

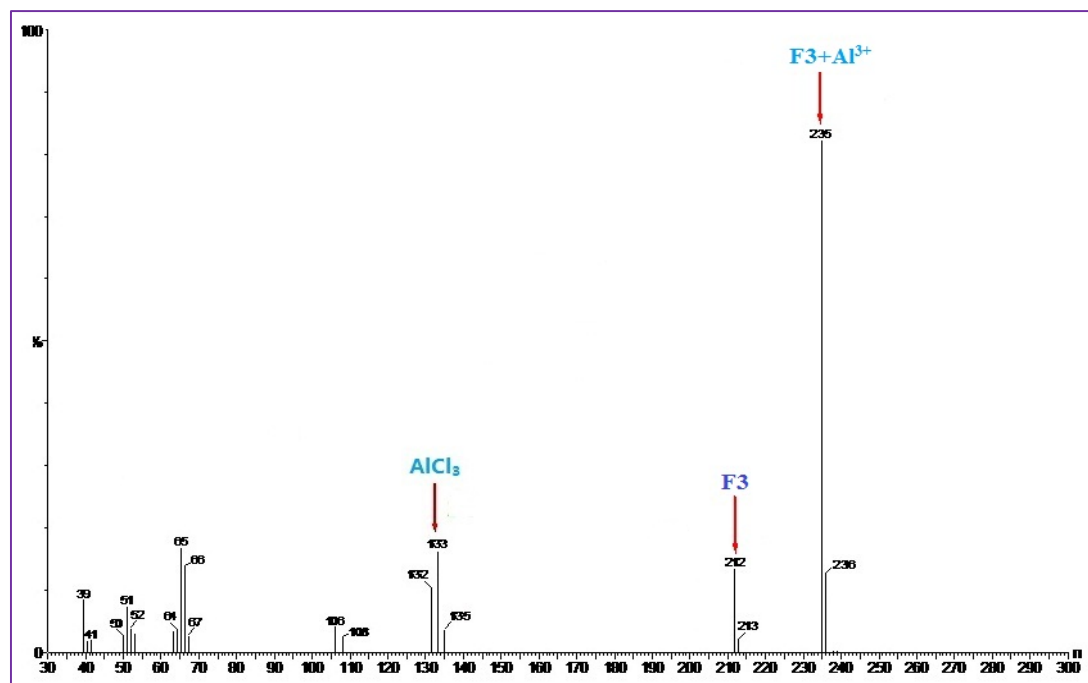


Fig. S36 Mass (FAB) spectral changes of **F3** (1 equiv.) + Al^{3+} (1 equiv.).

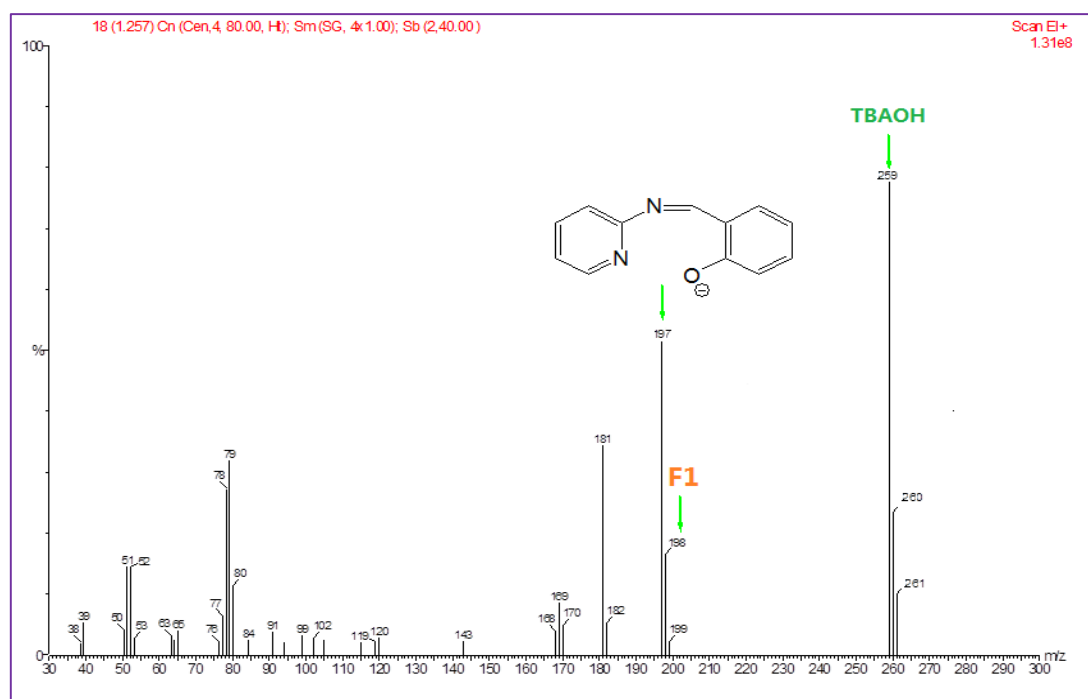


Fig. S37 Mass (FAB) spectral changes of **F1** (1 equiv.) + OH^- (5 equiv.).

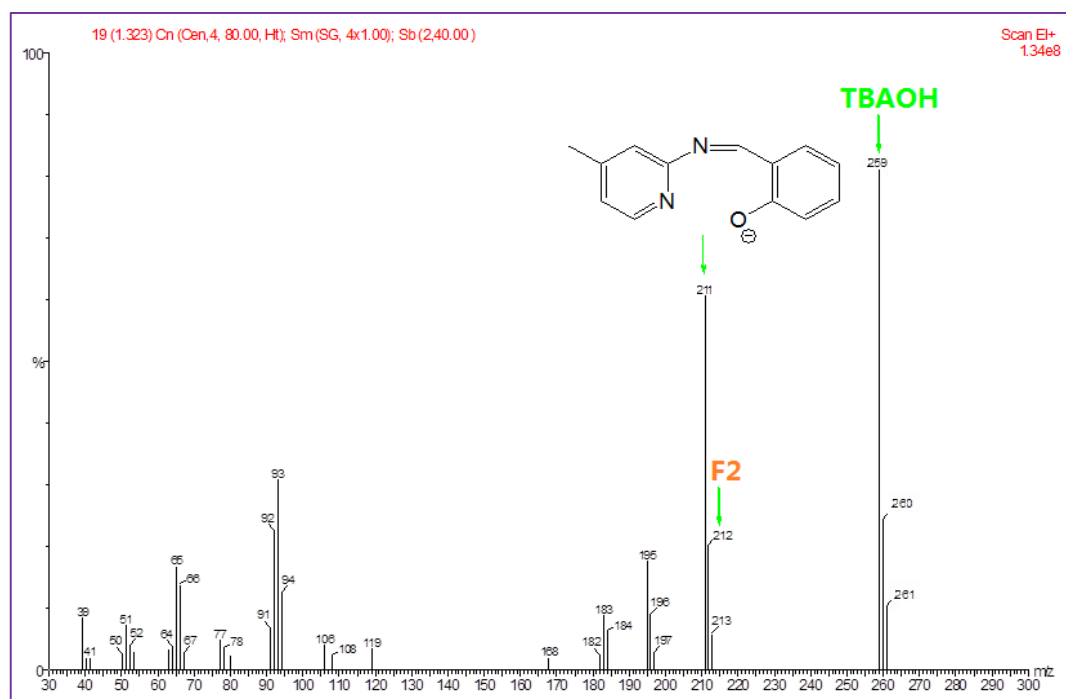


Fig. S38 Mass (FAB) spectral changes of **F2** (1 equiv.) + OH⁻ (5 equiv.).

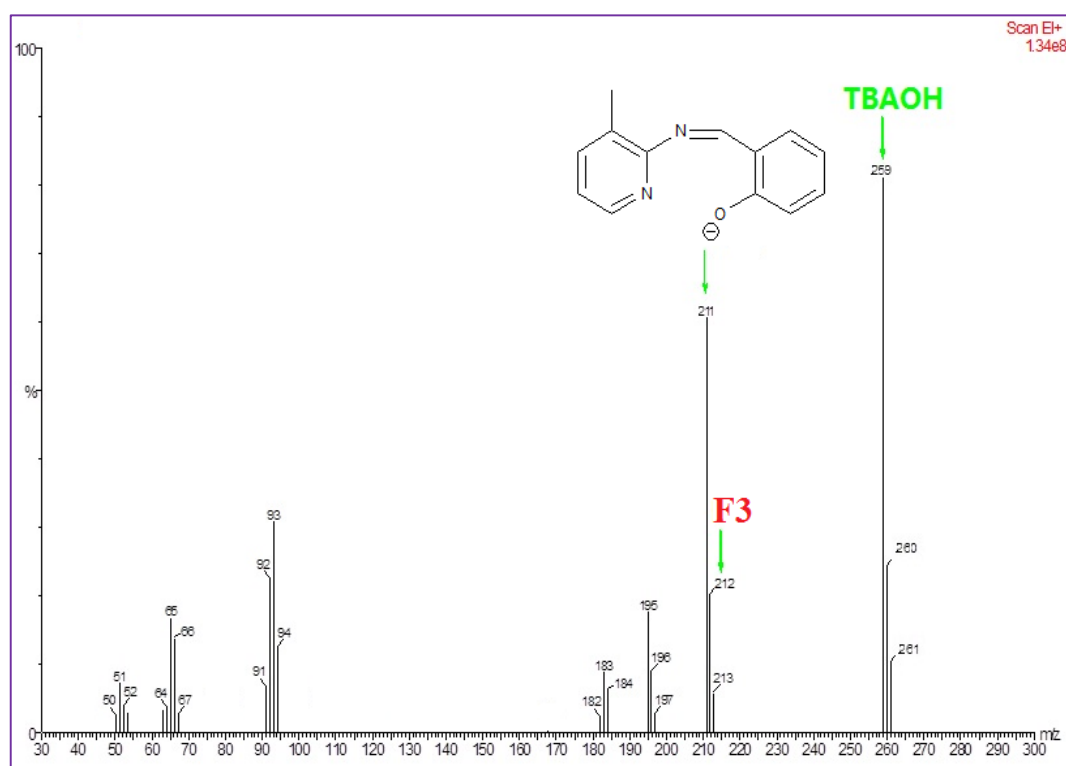


Fig. S39 Mass (FAB) spectral changes of **F3** (1 equiv.) + OH⁻ (5 equiv.).

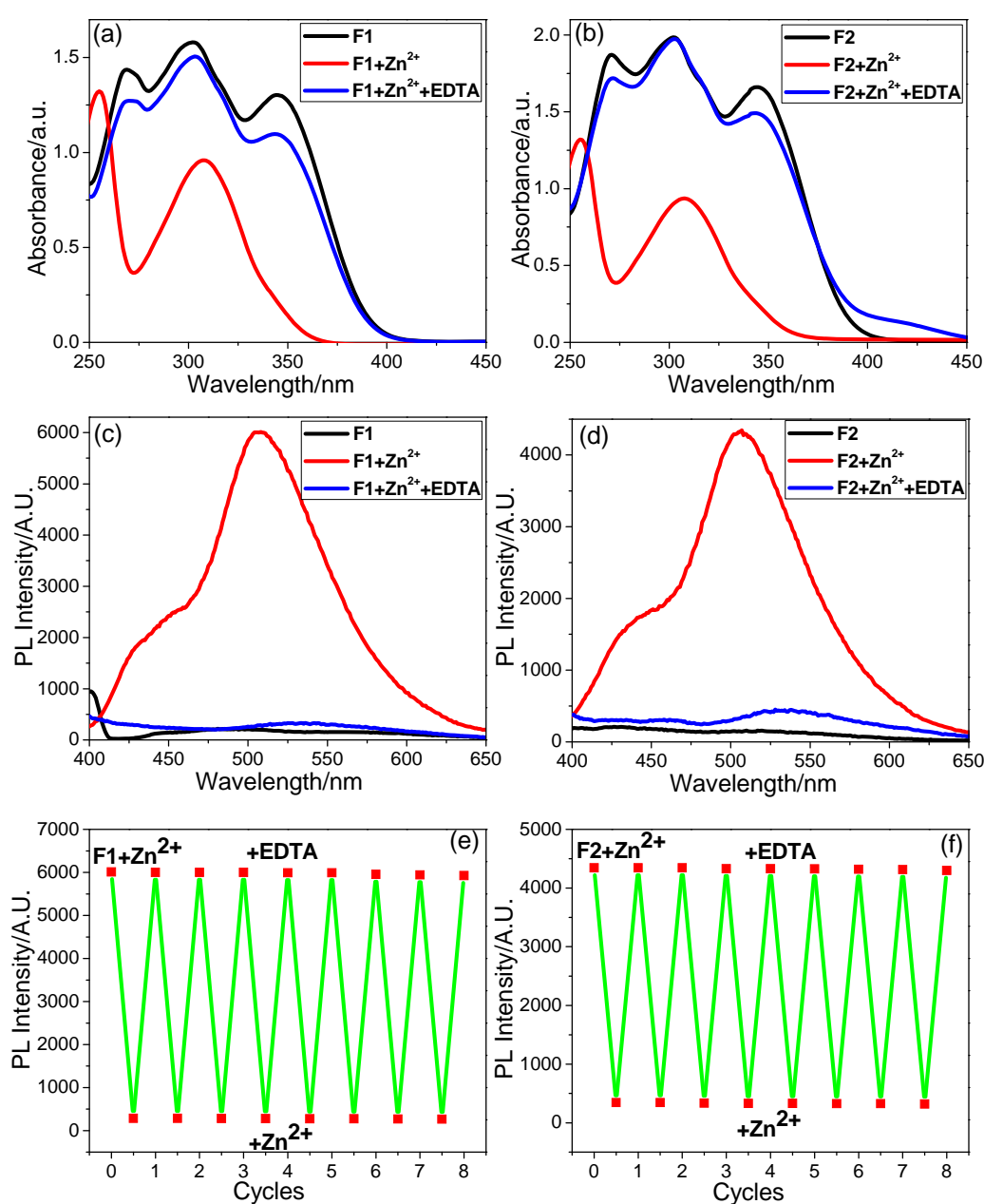


Fig. S40 UV-Vis absorption spectra (a, b), fluorescence spectra (c, d), and reversible cycles (e, f) for sensor reversibilities of $\mathbf{F1} + \text{Zn}^{2+}$ and $\mathbf{F2} + \text{Zn}^{2+}$, respectively.

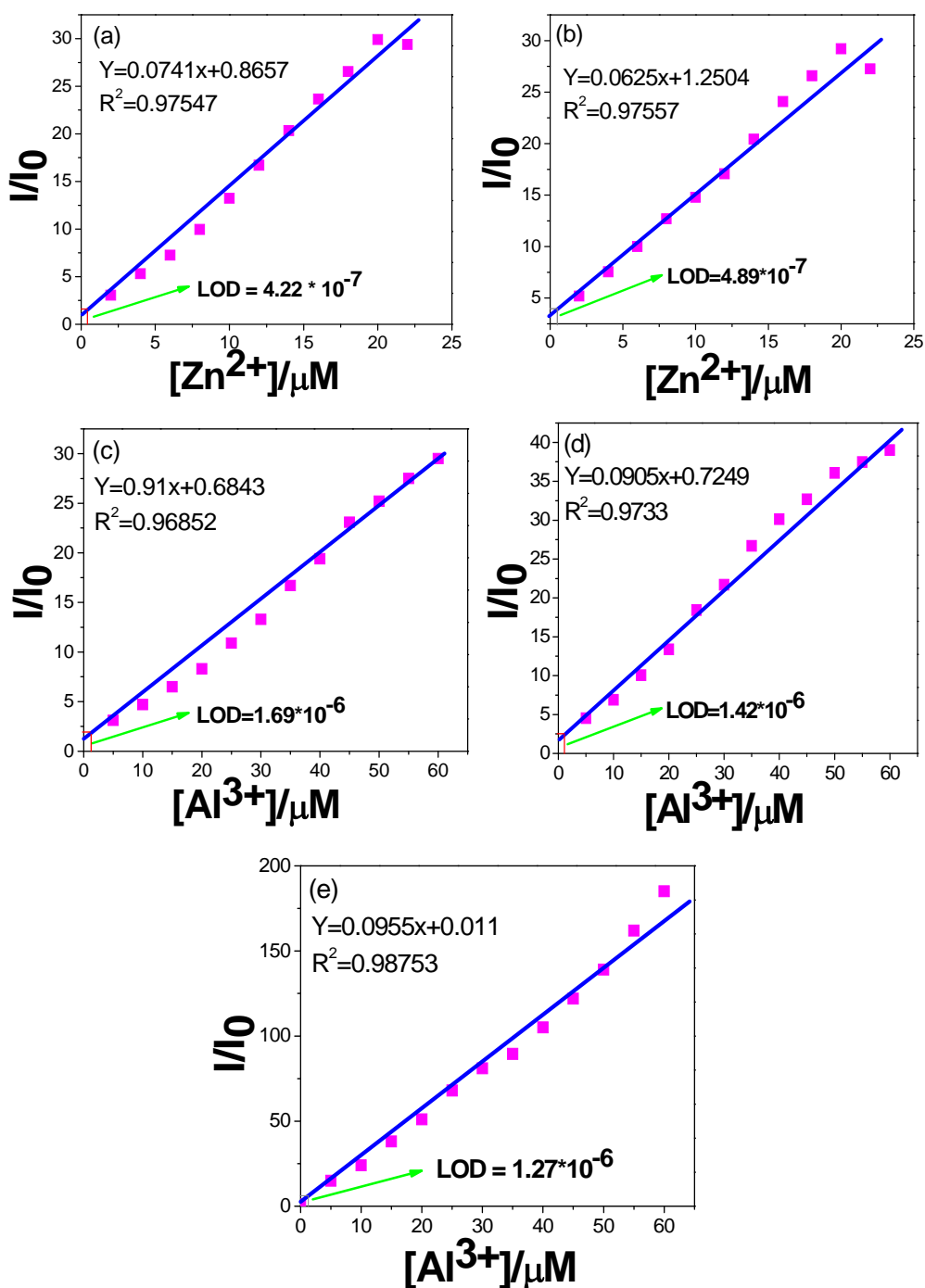


Fig. S41 Standard deviations and linear fit equations for detection limit calculations of (a) **F1** + Zn^{2+} , (b) **F2** + Zn^{2+} , (c) **F1** + Al^{3+} , (d) **F2** + Al^{3+} and (e) **F3** + Al^{3+} . [Note: Detection limit calculations were based on relative fluorescence intensity changes versus respective metal ion concentrations].

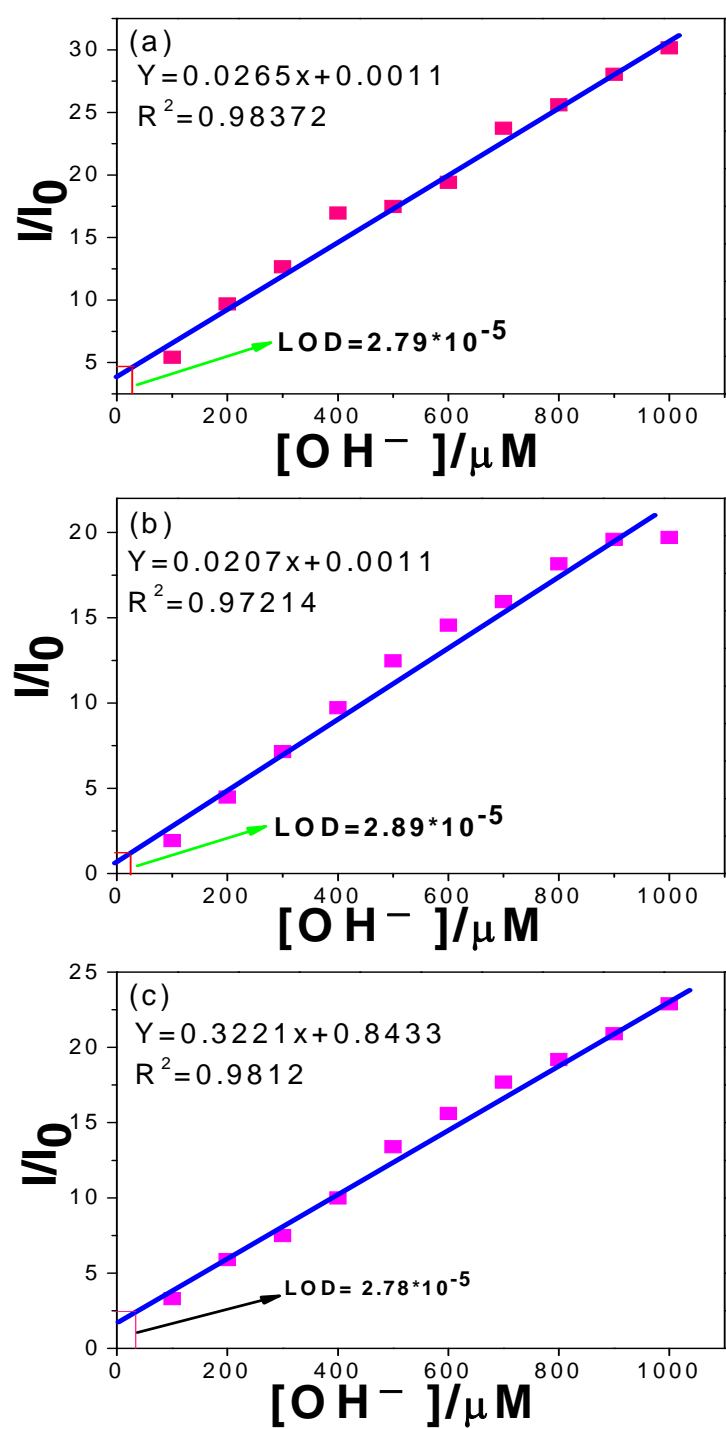


Fig. S42 Detection limits calculations of (a) $F1+OH^-$, (b) $F2+OH^-$, and (c) $F3+OH^-$, respectively, by standard deviations and linear fit equations.

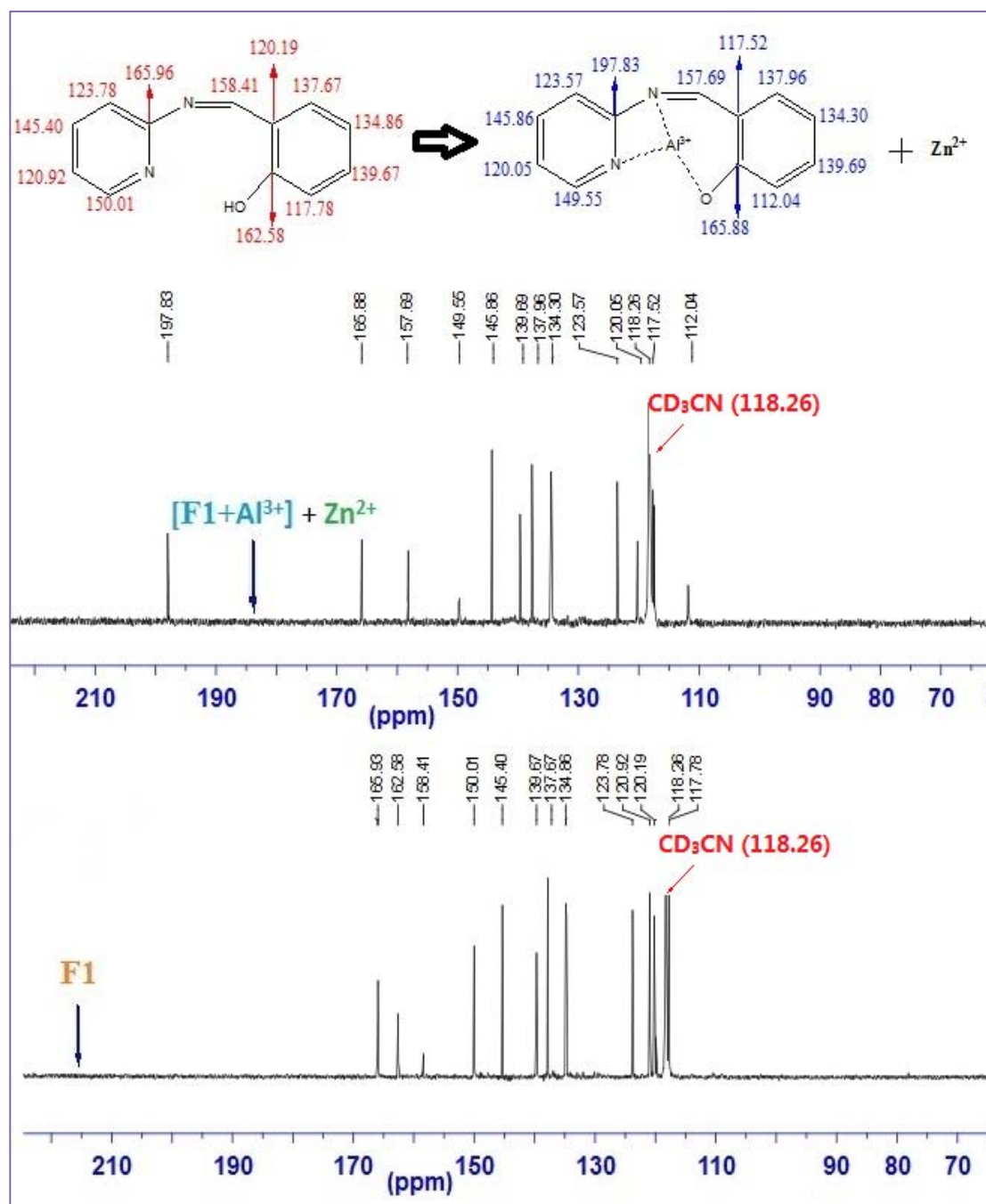


Fig. S43 ^{13}C NMR spectral changes of **F1** (1 equiv.) in CD_3CN with $(\text{Al}^{3+} + \text{Zn}^{2+})$ [(1:1) (each 3 equiv.)] in D_2O .

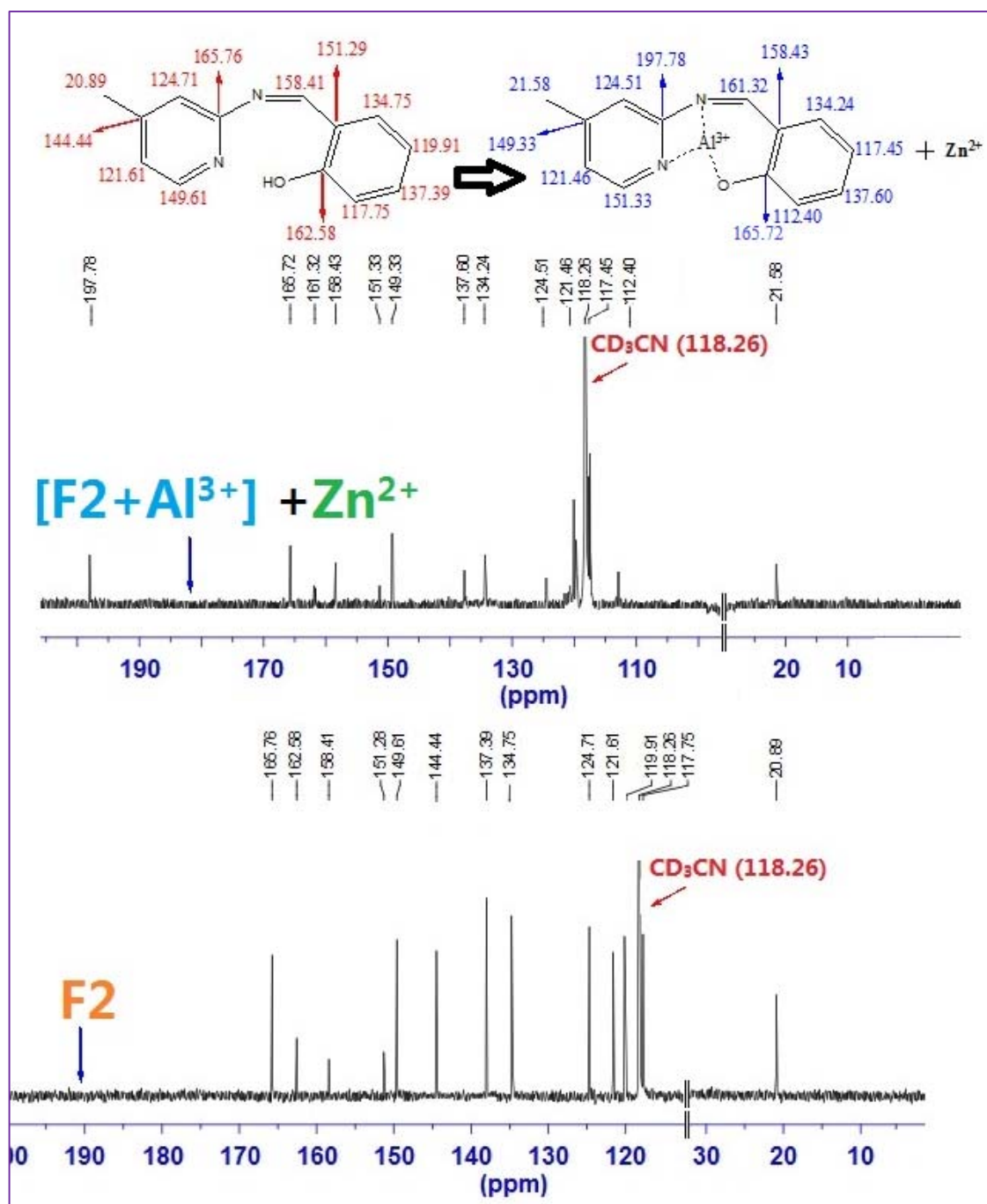


Fig. S44 ^{13}C NMR spectral changes of **F2** (1 equiv.) in CD_3CN with $(\text{Al}^{3+} + \text{Zn}^{2+})$ [(1:1) (each 3 equiv.)] in D_2O .

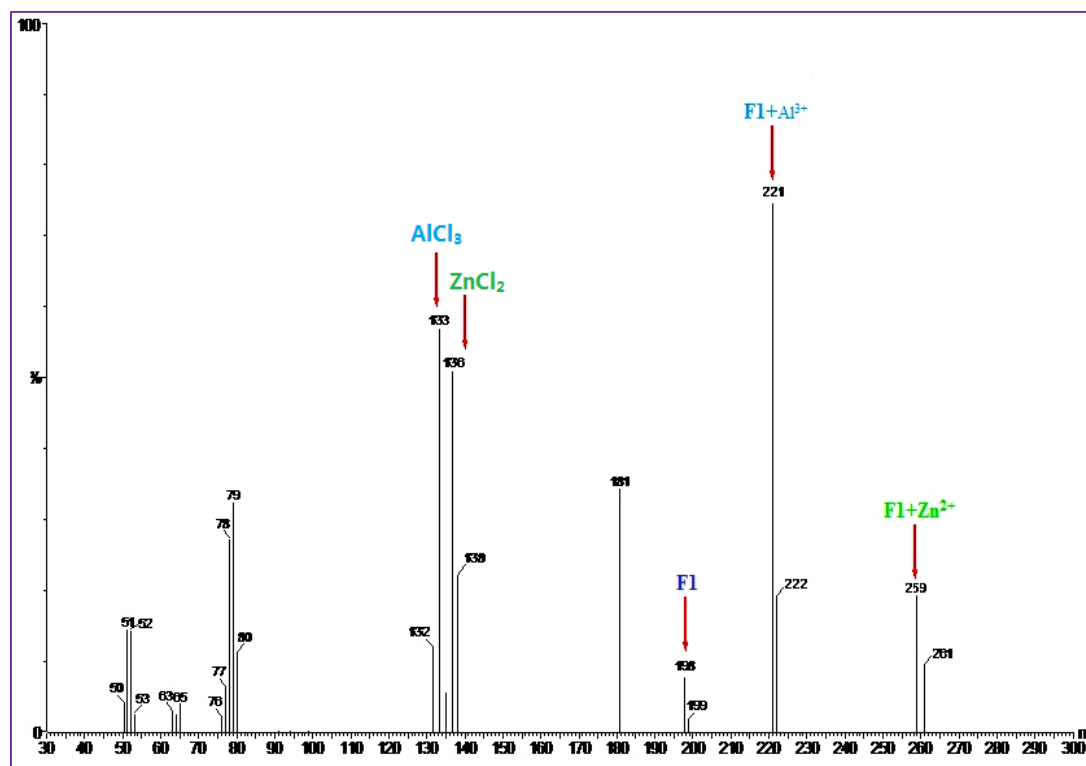


Fig. S45 Mass (FAB) spectral changes of **F1** (1 equiv.) + ($\text{Al}^{3+} + \text{Zn}^{2+}$) [(1:1) (each 3 equiv.)].

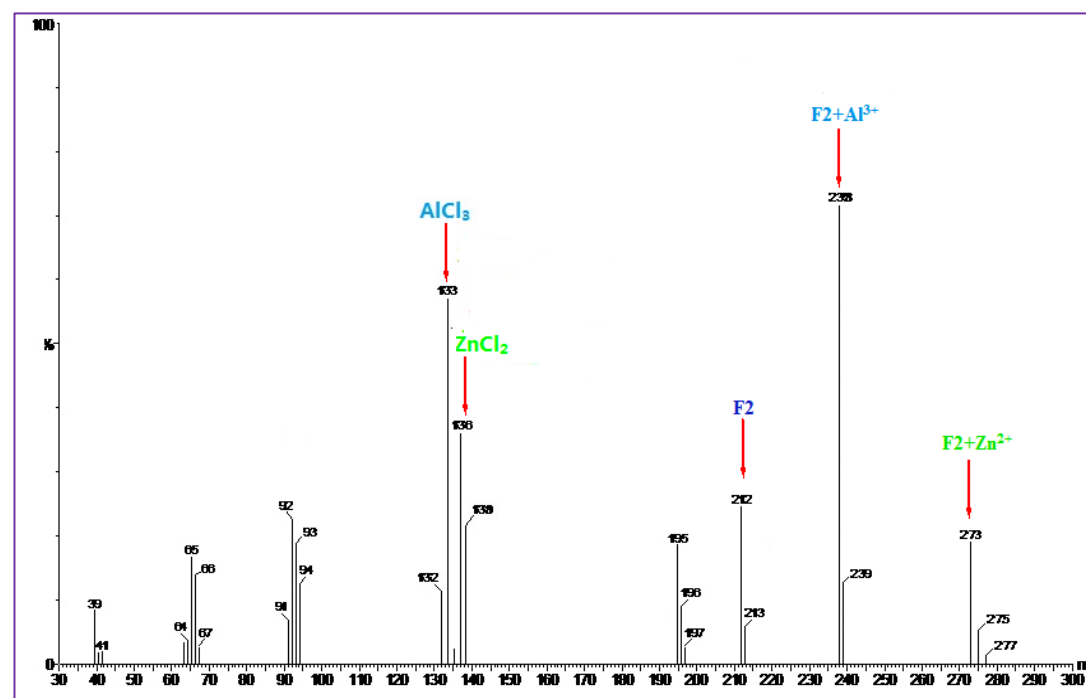


Fig. S46 Mass (FAB) spectral changes of **F2** (1 equiv.) + ($\text{Al}^{3+} + \text{Zn}^{2+}$) [(1:1) (each 3 equiv.)].

Response parameter and determination of binding constant^{2,3}

The response parameter α is defined as the ratio of the free ligand concentration to the initial concentration of the ligand. α defined as the ratio between the free ligand concentration ($[L]$) and the total concentration of ligand ($[L_T]$):

$$\alpha = \frac{[L]}{[L_T]}$$

α can be determined from the emission changes in the presence of different concentrations of M^{n+} :

$$\alpha = \frac{[I - I_0]}{[I_1 - I_0]}$$

where I_1 and I_0 are the limiting emission values for $\alpha = 1$ (in the absence of M^{n+}) and $\alpha = 0$ (probe is completely complexes with M^{n+}), respectively.

These equations² lead to the following equations that can be used in any stoichiometric ratio between the ligand and analyte.

$$[M^{n+}]^m = \frac{1}{nK} \cdot \frac{1}{[L]_T^{n-1}} \cdot \frac{1-\alpha}{\alpha^n}$$

Where K is complex equilibrium constant, $M_m L_n$ is metal-ligand, L is ligand, [L], $[M^{n+}]$, and $[M_m L_n]$ are the concentrations of respective species.

The stoichiometric ratio of the Zn^{2+} : fluorophore is 1:1. So, this equation can be written as

$$[Zn^{2+}] = \frac{1}{2KL} \cdot \frac{1-\alpha}{\alpha^2}$$

The stoichiometric ratio of the Al^{3+} : fluorophore is 1:1. So, this equation can be written as

$$[Al^{3+}] = \frac{1}{3KL^2} \cdot \frac{1-\alpha}{\alpha^3}$$

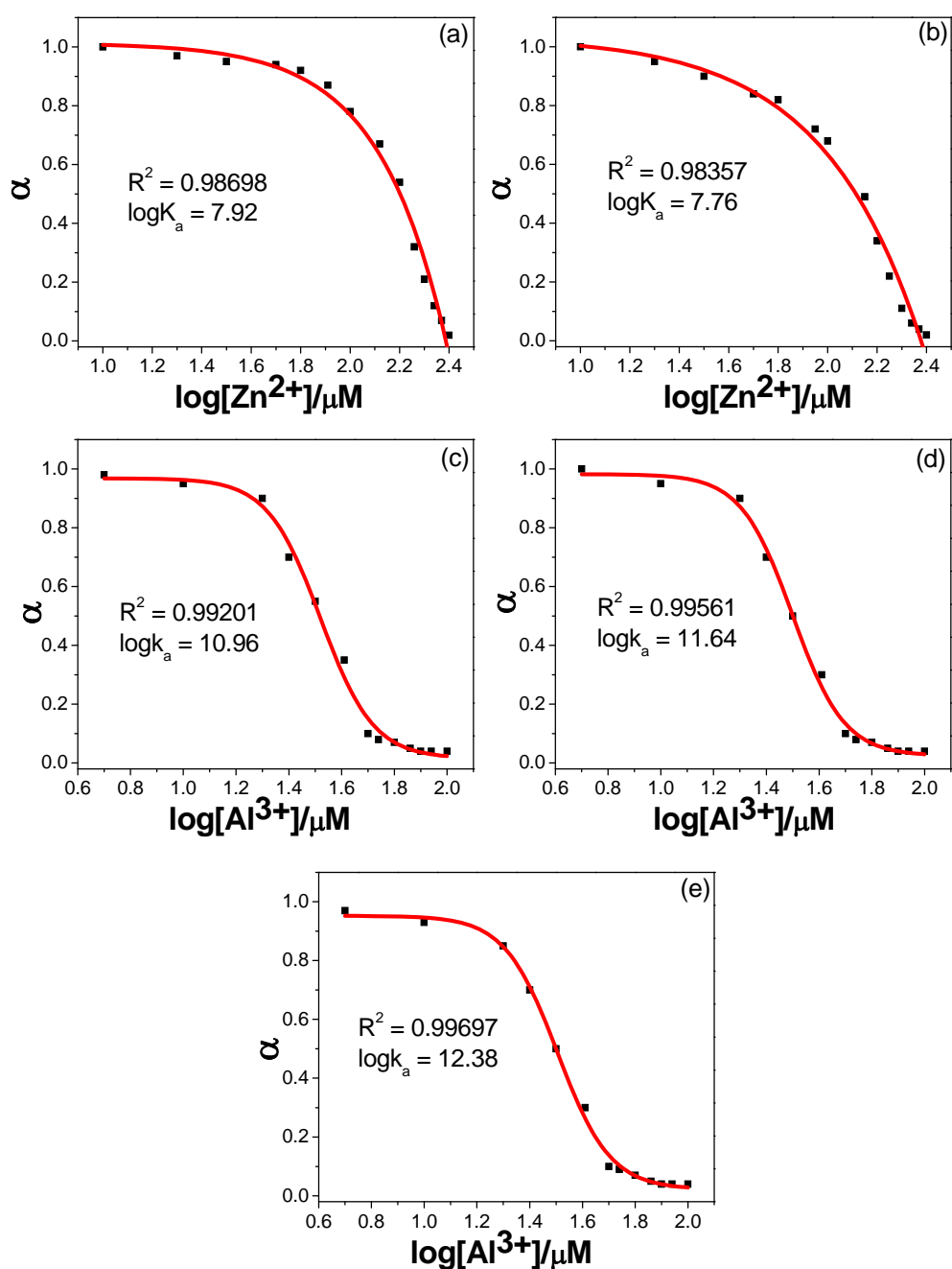


Fig. S47 Response parameter values (α) of (a) **F1** and (b) **F2** as a function of the logarithm of $[\text{Zn}^{2+}]$; (c) **F1**, (d) **F2**, and (e) **F3** as a function of the logarithm of $[\text{Al}^{3+}]$. α is defined as the ratio between the free ligand concentration $[L]$ and the initial concentration $[L_0]$ of ligand.

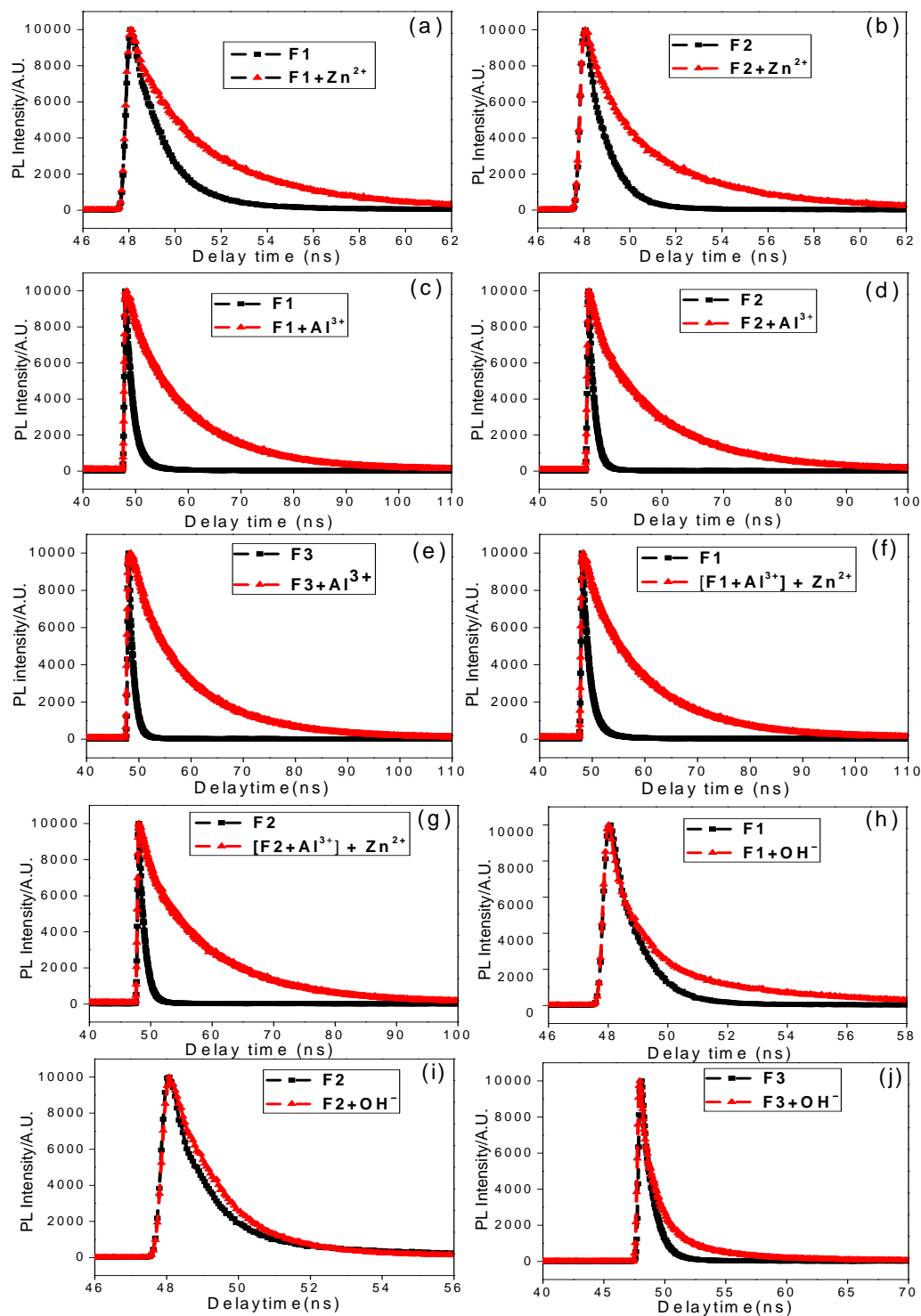


Fig. S48 Time-resolved fluorescence spectra of [F1 and F2 (1 equiv.) + Zn²⁺ (1 equiv.)] (a, b); [F1, F2 and F3 (1 equiv.) + Al³⁺ (3 equiv.)] (c, d, and e); [F1 or F2 (1 equiv.) + (Al³⁺+Zn²⁺) [(1:1) (each 3 equiv.)] (f, g); and [F1, F2 and F3 (1 equiv.) + OH⁻ (50 equiv.)] (h, i, and j)

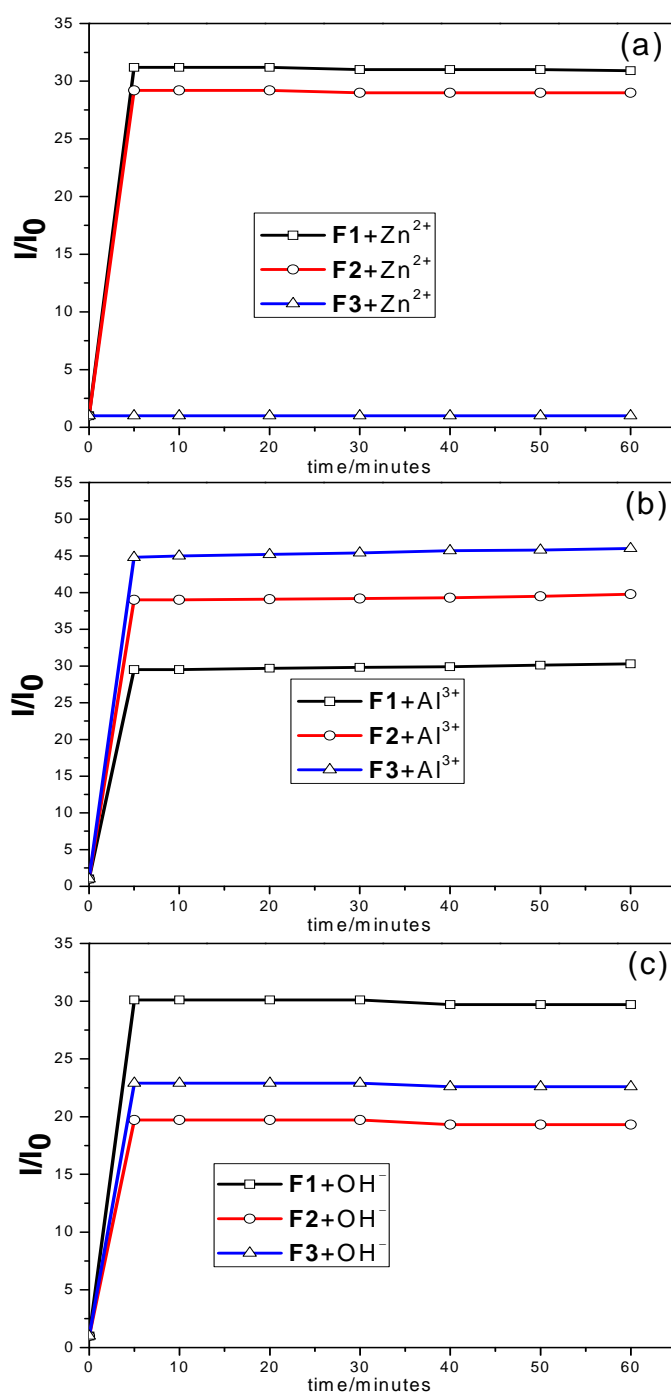


Fig. S49 PL spectral responses of (a) $\text{F1} + \text{Zn}^{2+}$, $\text{F2} + \text{Zn}^{2+}$ and $\text{F3} + \text{Zn}^{2+}$, (b) $\text{F1} + \text{Al}^{3+}$, $\text{F2} + \text{Al}^{3+}$ and $\text{F3} + \text{Al}^{3+}$, and (c) $\text{F1} + \text{OH}^-$, $\text{F2} + \text{OH}^-$ and $\text{F3} + \text{OH}^-$ as a function of time (0-60 minutes).

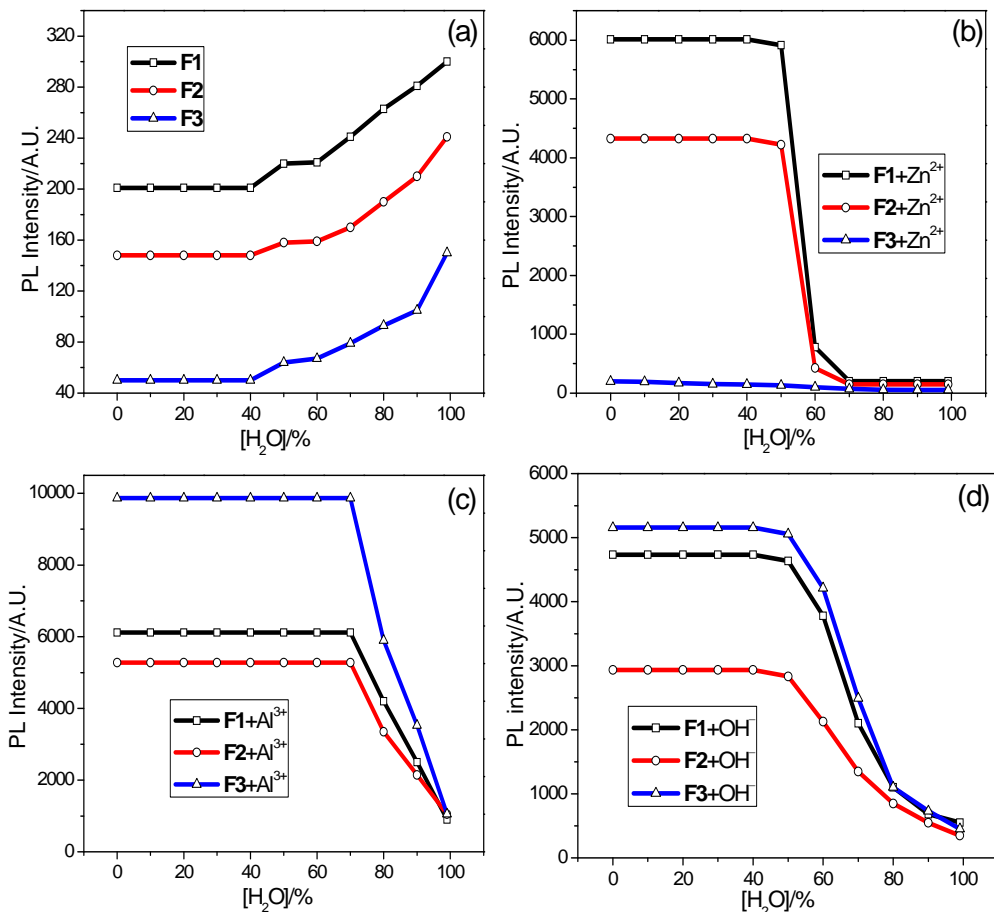


Fig. S50 PL spectral responses of (a) **F1**, **F2** and **F3**, (b) **F1+Zn²⁺**, **F2+Zn²⁺** and **F3+Zn²⁺**, (c) **F1+Al³⁺**, **F2+Al³⁺** and **F3+Al³⁺**, (d) **F1+OH⁻**, **F2+OH⁻** and **F3+OH⁻** as a function of increasing water concentration (0-99%).

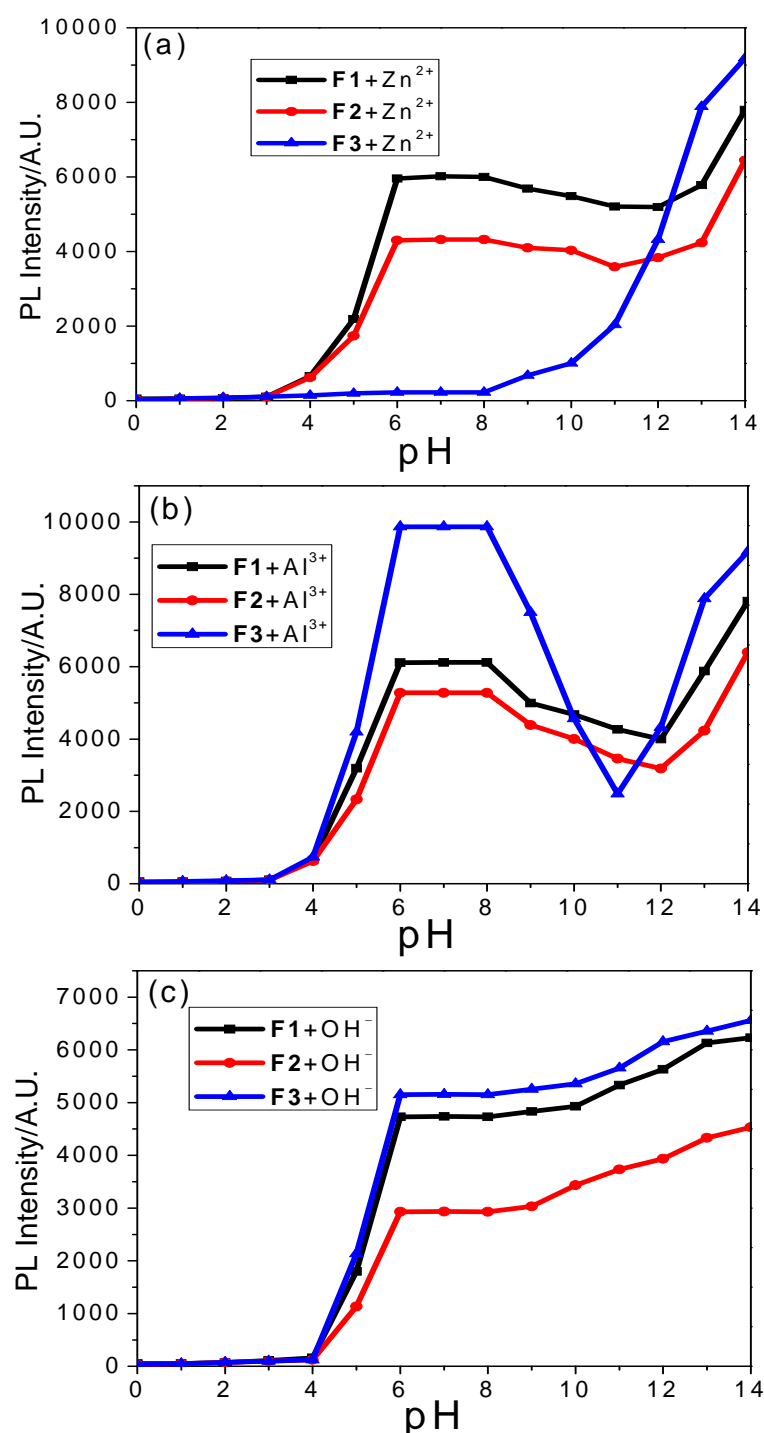


Fig. S51 PL spectral responses of (a) $\text{F1} + \text{Zn}^{2+}$, $\text{F2} + \text{Zn}^{2+}$ and $\text{F3} + \text{Zn}^{2+}$, (b) $\text{F1} + \text{Al}^{3+}$, $\text{F2} + \text{Al}^{3+}$ and $\text{F3} + \text{Al}^{3+}$, (c) $\text{F1} + \text{OH}^{-}$, $\text{F2} + \text{OH}^{-}$ and $\text{F3} + \text{OH}^{-}$ as a function of pH (0-14).

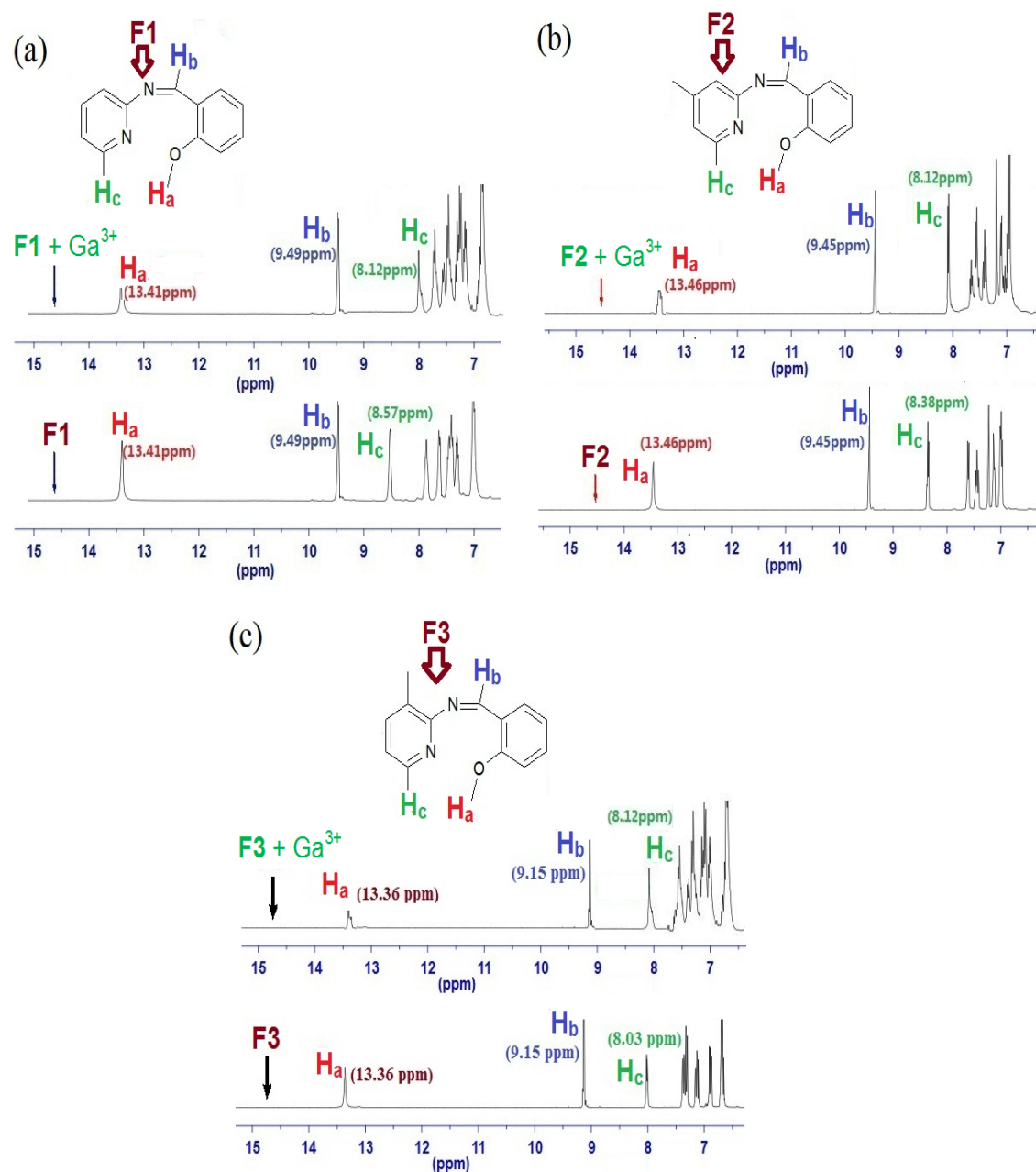


Fig. S52 ¹H NMR spectral changes of (a) **F1** (1 equiv.) in CD₃CN (b) **F2** (1 equiv.) in CD₃CN with Ga³⁺ ions (5 equiv.) in D₂O.

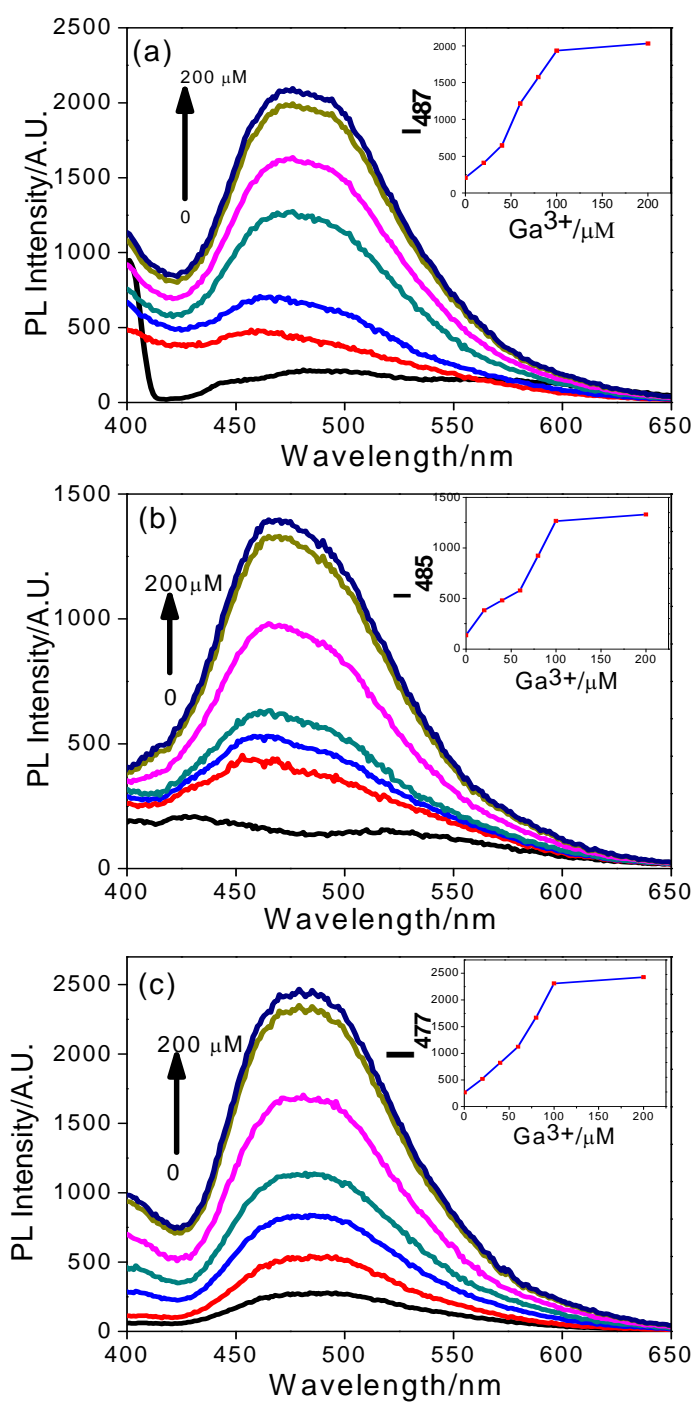


Fig. S53 Fluorescence spectral changes of (a) **F1** (1×10^{-5} M) in $\text{CH}_3\text{CN}/\text{H}_2\text{O}$ (6/4; vol/vol) ($\lambda_{\text{ex}}=344$ nm), (b) **F2** (1×10^{-5} M) in $\text{CH}_3\text{CN}/\text{H}_2\text{O}$ (6/4; vol/vol) ($\lambda_{\text{ex}}=346$ nm), and (c) **F3** (1×10^{-5} M) in $\text{CH}_3\text{CN}/\text{H}_2\text{O}$ (6/4; vol/vol) ($\lambda_{\text{ex}}=343$ nm) titrated with 0–60 μM of Al^{3+} ions in H_2O (0, 20, 40, 60, 80, 100 and 200 μM were plotted). Insets show PL spectral responses of (a) **F1**, (b) **F2** and (c) **F3** as a function of Ga^{3+} .

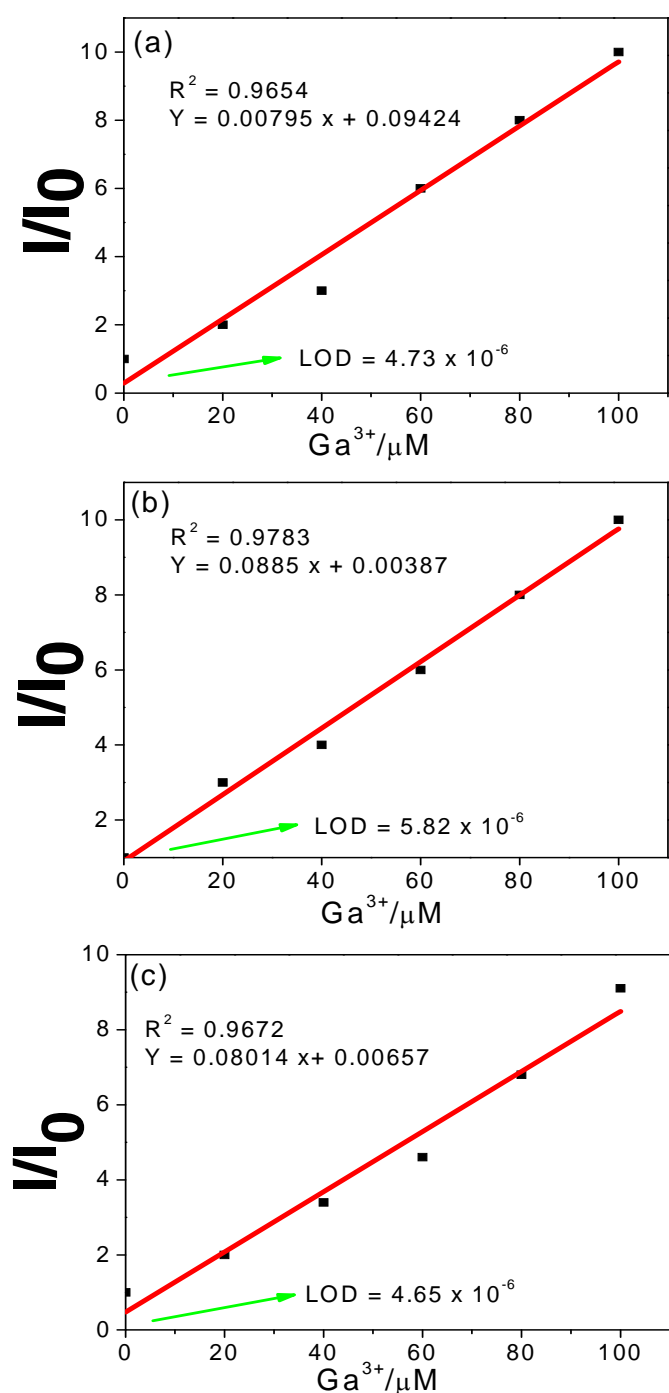


Fig. S54 Standard deviations and linear fit equations for detection limit calculations of (a) **F1** + Ga^{3+} , (b) **F2** + Ga^{3+} and (c) **F3** + Ga^{3+} . [Note: Detection limit calculations were based on relative fluorescence intensity changes versus respective metal ion concentrations].

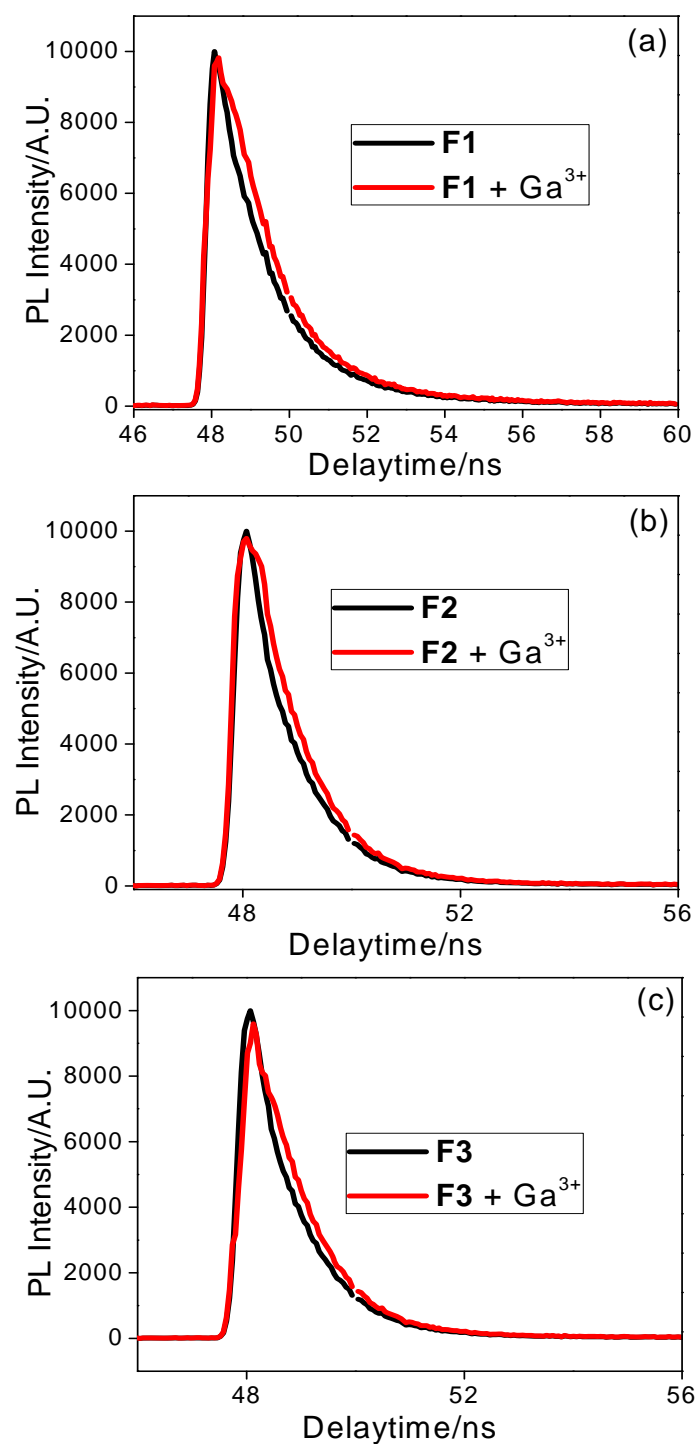


Fig. S55 TRPL spectra of (a) $\mathbf{F1} + \text{Ga}^{3+}$, (b) $\mathbf{F2} + \text{Ga}^{3+}$ and (c) $\mathbf{F3} + \text{Ga}^{3+}$.

Table S1 Photophysical properties of sensor complexes.

Sensor Complexes	Φ	^{a, c} Association Constants (log K _a)	^a Detection	
			Limits (LODs/M)	^{a, d} τ (ns)
F1+Zn²⁺	0.281 ^a	7.92	4.22x10 ⁻⁷	4.15
F1+Al³⁺	0.291 ^{a, b}	10.96	1.69x10 ⁻⁶	11.97
[F1+Al³⁺] + Zn ²⁺	0.286 ^a	NA	NA	11.78
F1+OH⁻	0.220 ^a	NA	2.79x10 ⁻⁵	3.95
F1+Ga³⁺	0.072	NA	4.73x10 ⁻⁶	2.65
F2+Zn²⁺	0.196 ^a	7.76	4.89x10 ⁻⁷	3.83
F2+Al³⁺	0.221 ^{a, b}	11.64	1.42x10 ⁻⁶	11.52
[F2+Al³⁺] + Zn ²⁺	0.214 ^a	NA	NA	11.47
F2+OH⁻	0.122 ^a	NA	2.89x10 ⁻⁵	2.28
F2+Ga³⁺	0.064	NA	5.82x10 ⁻⁶	1.76
F3+Al³⁺	0.307 ^{a, b}	12.38	1.27x10 ⁻⁶	12.16
F3+OH⁻	0.171 ^a	NA	2.78x10 ⁻⁵	2.18
F3+Ga³⁺	0.076	NA	4.65x10 ⁻⁶	1.54

^aCH₃CN/H₂O (6/4), ^bCH₃CN/H₂O (3/7), 9-10 DPA in CH₃CN as a reference standard ($\Phi = 0.9$) and ^c[Zn²⁺] = 1/2K_aL (1- α / α^2) and [Al³⁺] = 1/3K_aL² (1- α / α^3); where L is the ligand and α = ratio between the free ligand concentration [L] and the initial concentration of ligand [L₀], ^dFluorescence lifetimes.

Table S2 TRPL decay constants of **F1**, **F2**, and **F3** in the presence of Zn^{2+} , Al^{3+} and OH^- ions.

Compound	τ_1 (ns)	τ_2 (ns)	A_1 (%)	A_2 (%)	τ_{Avg} (ns)
F1	1.38 ^a	8.93 ^a	89.2 ^a	10.8 ^a	2.19 ^a
	0.67 ^b	6.18 ^b	93.58 ^b	6.42 ^b	1.02 ^b
	1.55 ^c	5.91 ^c	27.6 ^c	72.4 ^c	3.85 ^c
F1+Zn²⁺	2.59	5.58	27.5	72.5	4.15
F1+Al³⁺	12.44	3.73	5.4	96.6	11.97
[F1+Al³⁺] + Zn ²⁺	11.68	3.71	6.8	93.2	11.78
F1+OH⁻	1.49	4.90	37.2	62.8	3.95
F1+Ga³⁺	1.67	6.72	76.2	23.8	2.65
F2	0.91 ^a	13.09 ^a	95.1 ^a	4.9 ^a	1.51 ^a
	0.71 ^b	7.66 ^b	95.25 ^b	4.75 ^b	1.04 ^b
	0.29 ^c	6.95 ^c	30.40 ^c	69.6 ^c	4.12 ^c
F2+Zn²⁺	1.55	4.71	27.6	72.4	3.83
F2+Al³⁺	12.08	2.28	5.1	94.9	11.52
[F2+Al³⁺] + Zn ²⁺	12.00	2.04	4.9	95.1	11.47
F2+OH⁻	0.99	5.74	44.6	55.4	2.28
F2+Ga³⁺	0.78	12.67	87.3	12.7	1.76
F3	0.88 ^a	13.48 ^a	98.1 ^a	1.9 ^a	1.35 ^a
	0.70 ^b	9.65 ^b	97.01 ^b	2.92 ^b	0.96 ^b
	0.51 ^c	6.68 ^c	27.72 ^c	72.28 ^c	3.59 ^c
F3+Al³⁺	14.07	5.95	4.1	95.9	12.16
F3+OH⁻	1.39	4.24	34.6	65.4	2.18
F3+Ga³⁺	0.92	11.56	85.6	14.4	1.54

^apH=7, ^bpH=2 and ^cpH=12.